رادیواپسیتی ها در فکین

رادیواپسیتی های آناتومیک در فکین

- سپتوم بینی
- سایه بینی
- Ant nasal spine


A

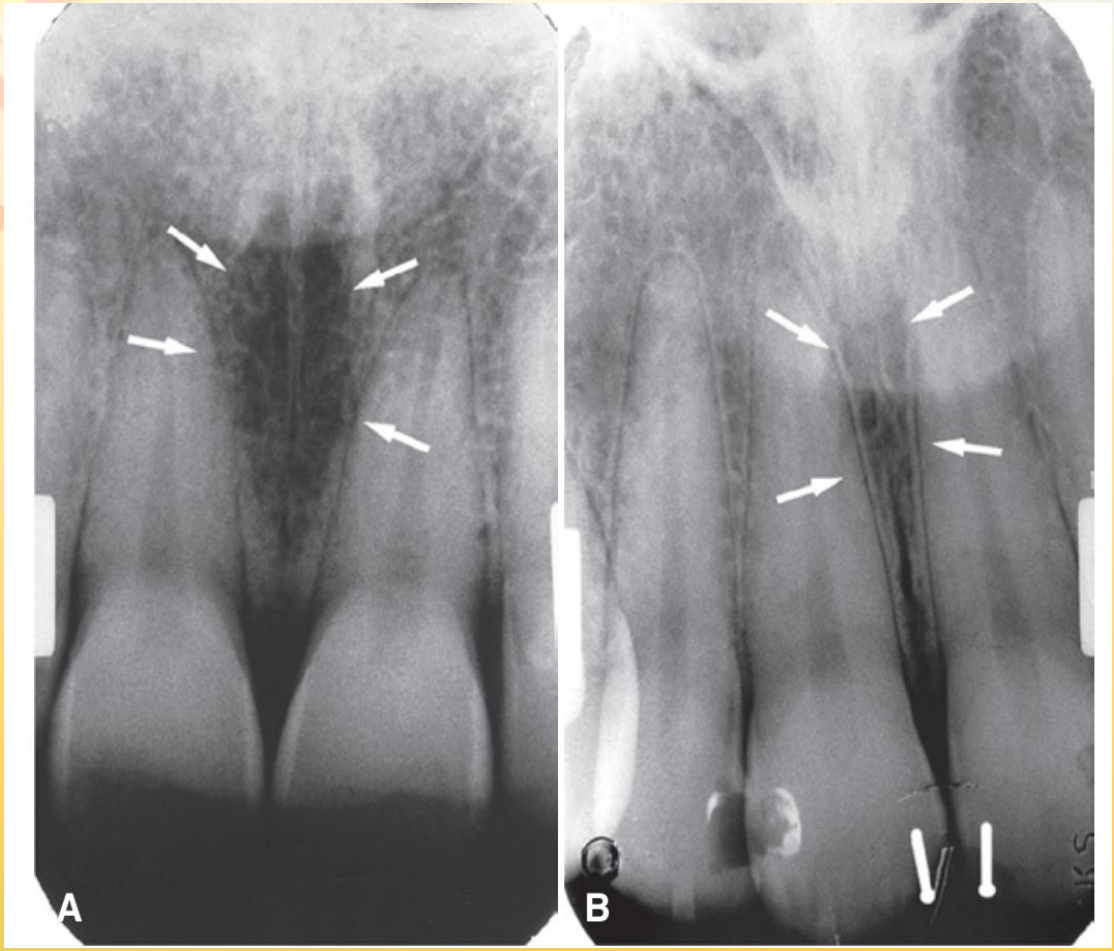
A
B

بوردر بینی و سینوس

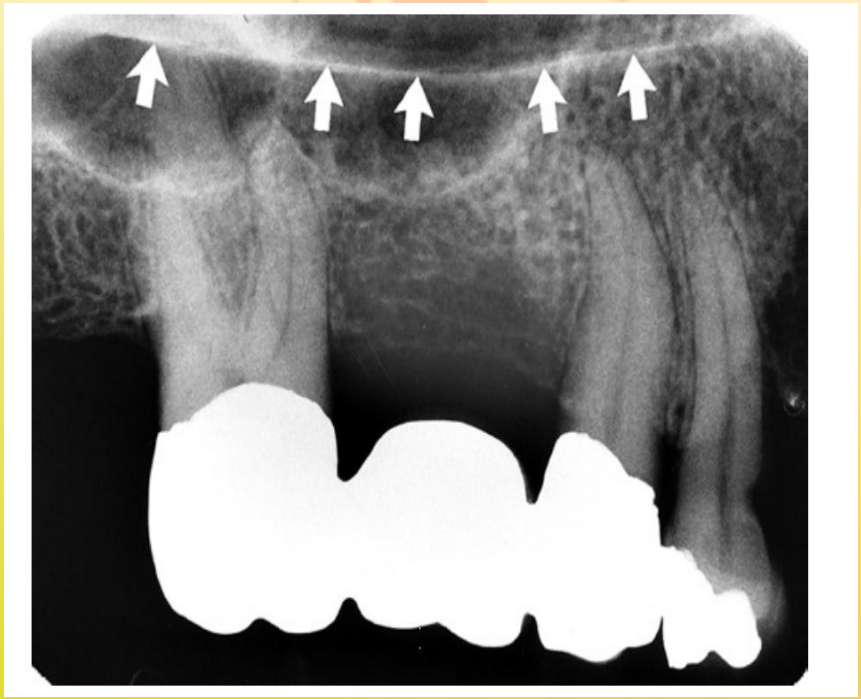

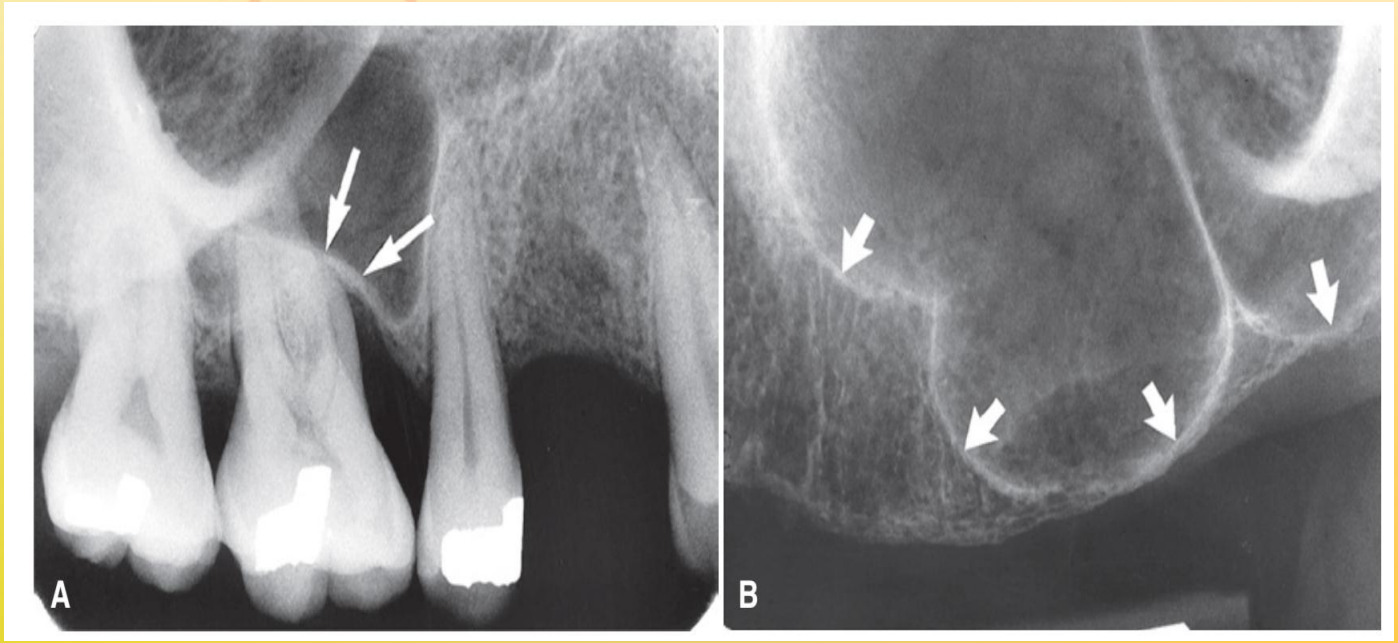
A
B

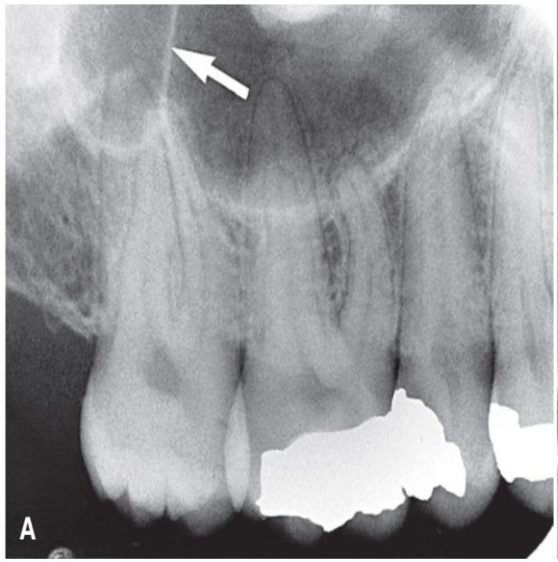

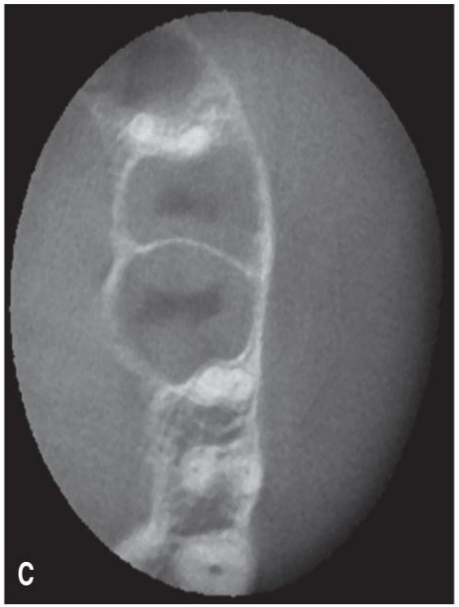

Fig. 12.41 Maxillary sinus septa. (A) Septum *(arrow)* in the maxillary sinus formed by a low ridge of bone on the sinus wall (see also Fig. 12.38B and 12.40). (B) Sagittal section shows septa in the region of the missing first molar (different patient than A). Note also thickening of the sinus mucous membrane. (C) Axial section of B at the level of the septum shows extension of septa from the buccal to palatal wall of the sinus.

زایگوماتیک پروسس ماگزیلا

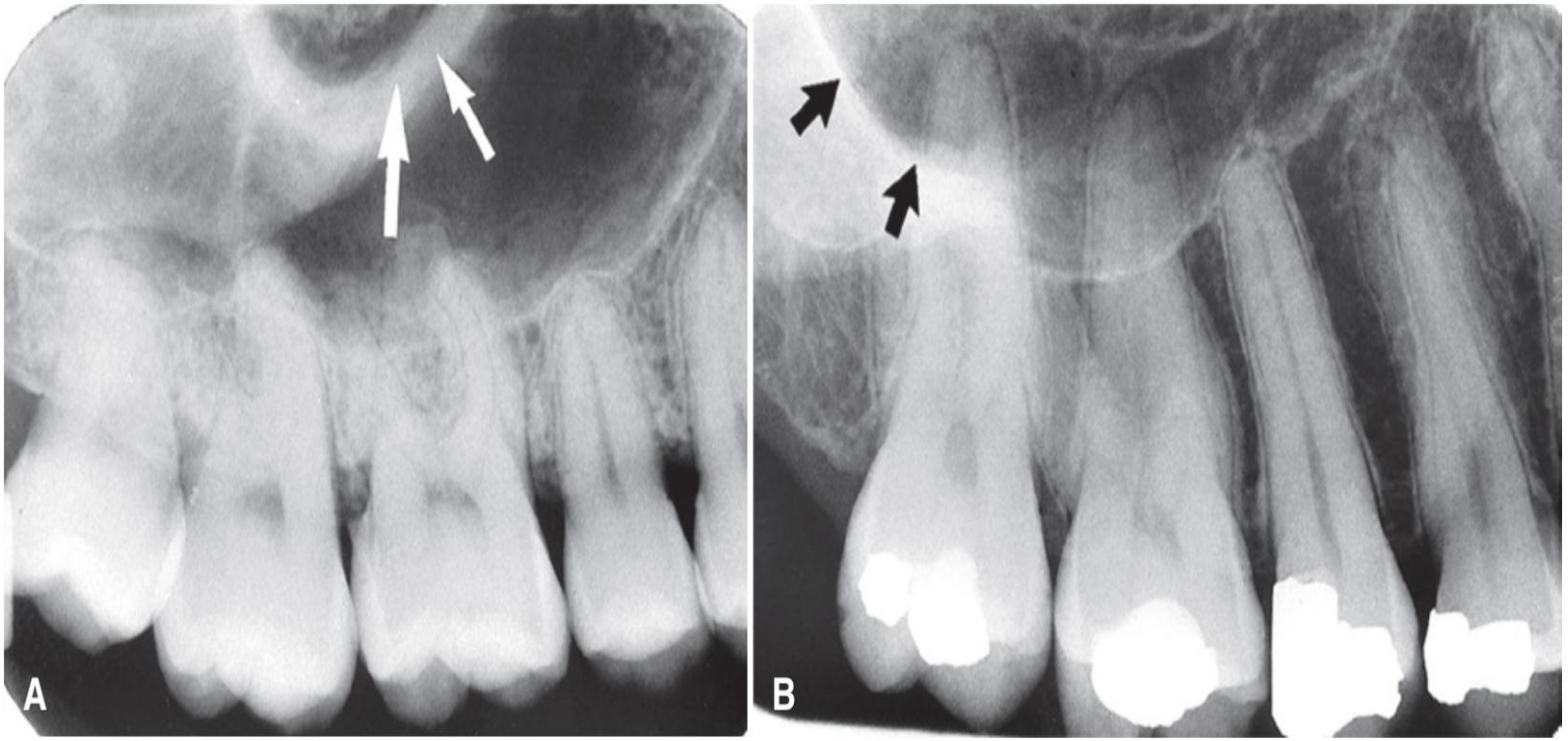

Fig. 12.43 The zygomatic process of the maxilla *(arrows)* protrudes laterally from the maxillary wall. Its size may be quite variable: small with thick borders (A) or large with thin borders (B).

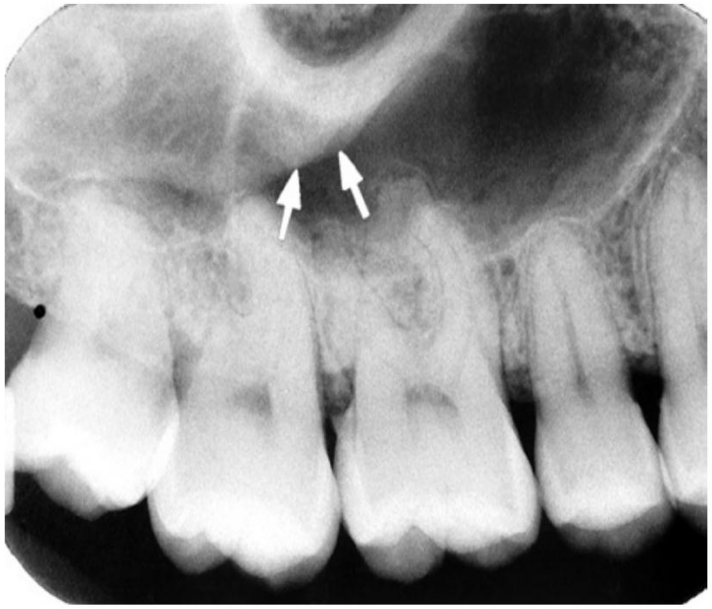

Fig. 12.44 The inferior border of the zygoma *(arrows)* extends posteriorly from the inferior portion of the zygomatic process of the maxilla.

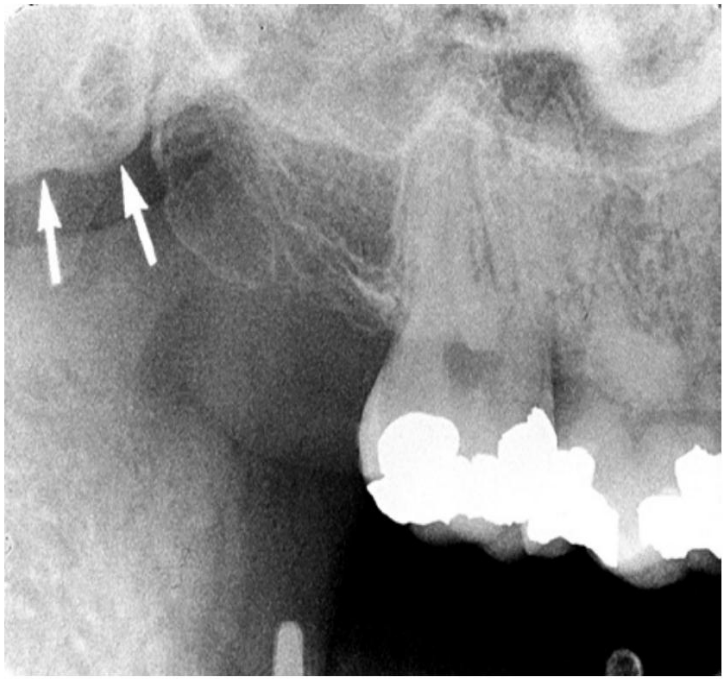

Fig. 12.46 Pterygoid plates *(arrows)* located posterior to the maxillary tuberosity.

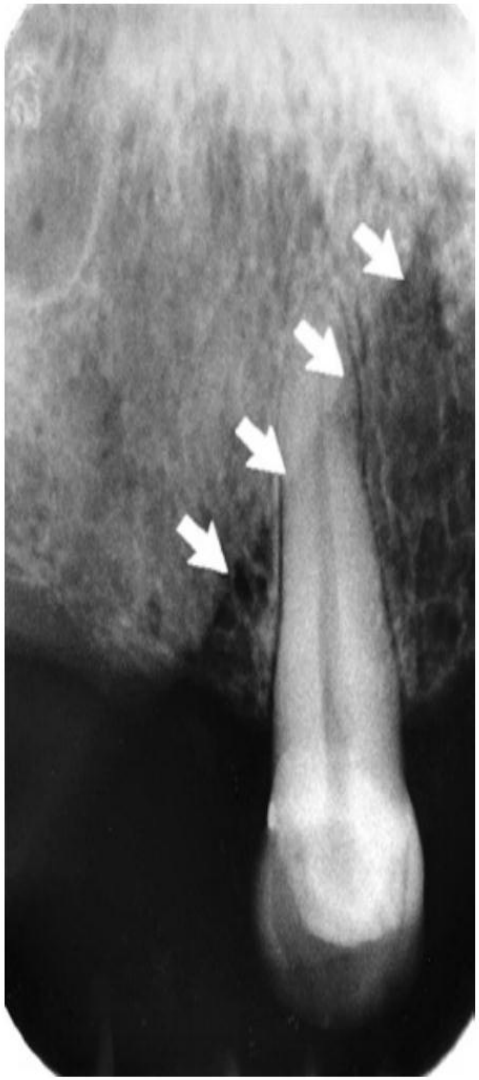

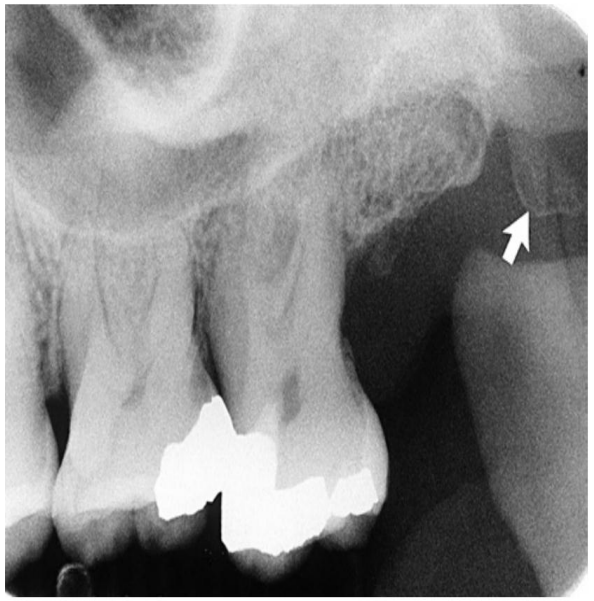

Fig. 12.47 The hamular process *(arrow)* extends inferiorly from the medial pterygoid plate.

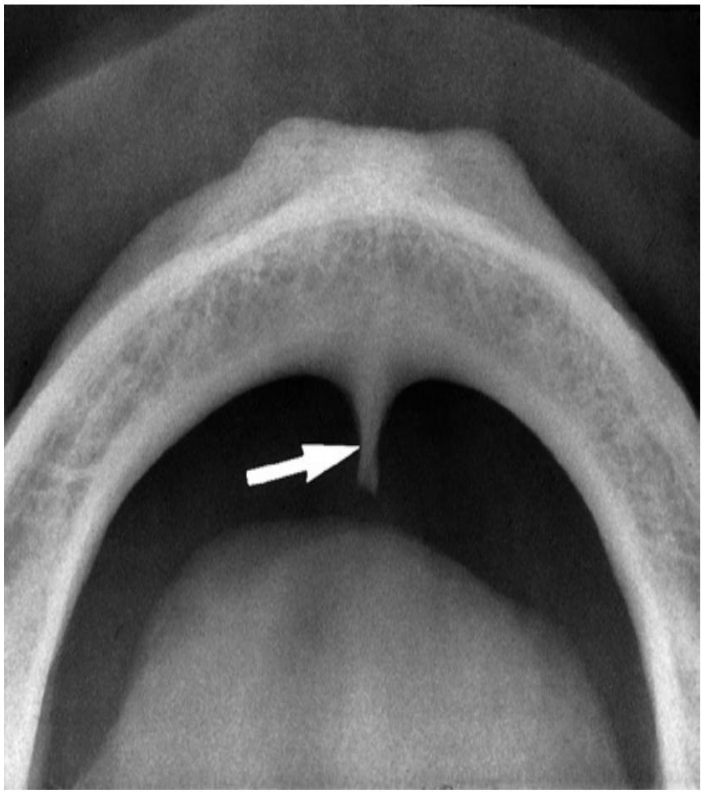

Fig. 12.49 Genial tubercle *(arrow)* on the lingual surface of the mandible in this cross-sectional mandibular occlusal view. This tubercle is unusually prominent.

ig. 12.65 External oblique ridge *(arrows)* on the buccal surface of the handible, seen as a radiopaque line near the alveolar crest in the mandibular ird molar region.

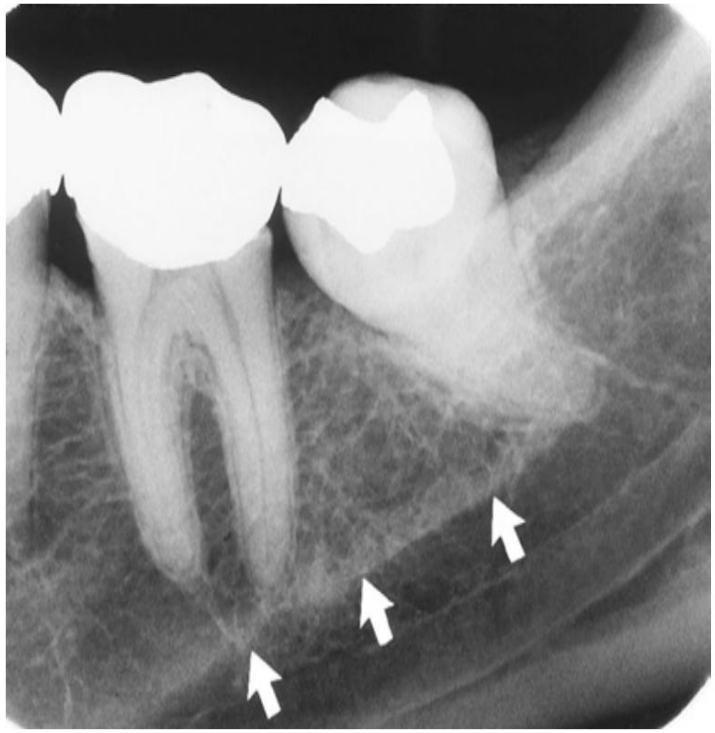

Fig. 12.62 Mylohyoid ridge *(arrows)* running at the level of the molar apices and above the inferior alveolar canal.

Fig. 12.67 Coronoid process of the mandible *(arrows)* superimposed on the maxillary tuberosity.

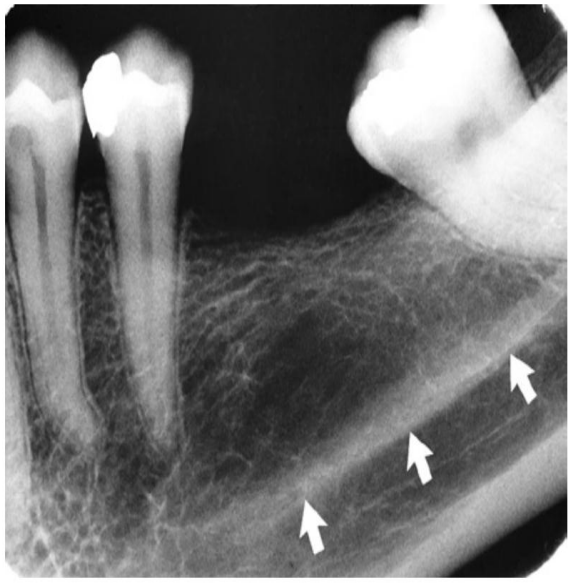

Fig. 12.63 The mylohyoid ridge *(arrows)* may be dense, especially when a radiograph is exposed with excessive negative angulation.

رادیواپسیتی های پری اپیکال

- کاندنسینگ اوستئیت
- پری اپیکال سمنتواسئوس دیسپلازی
- ایدیوپاتیک استئواسکلروزیس
- جسم خارجی
- هایپرسمنتوزیس

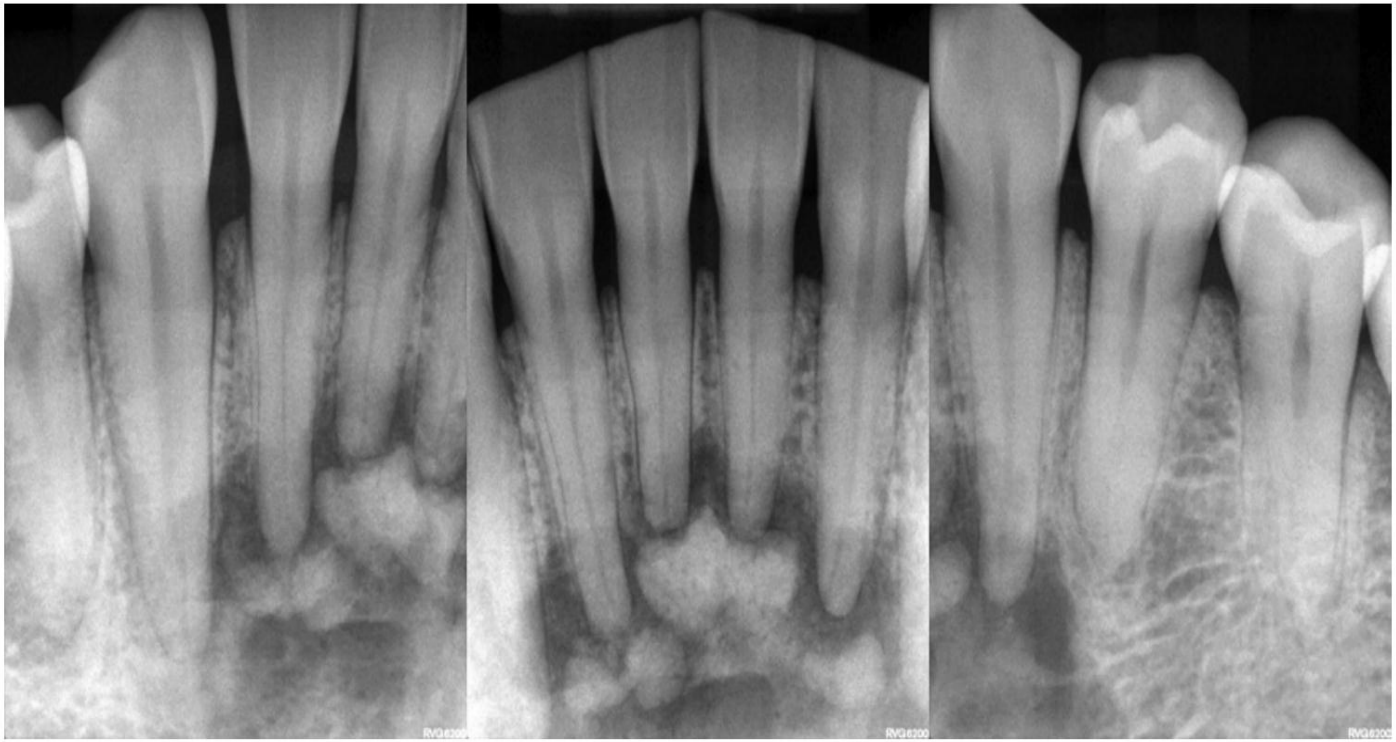

Fig. 25.22 The mixed radiolucent and radiopaque appearance of a more mature stage of periapical cemento-osseous dysplasia. Note the radiolucent rim encircling the radiopaque foci of dysplastic bone.

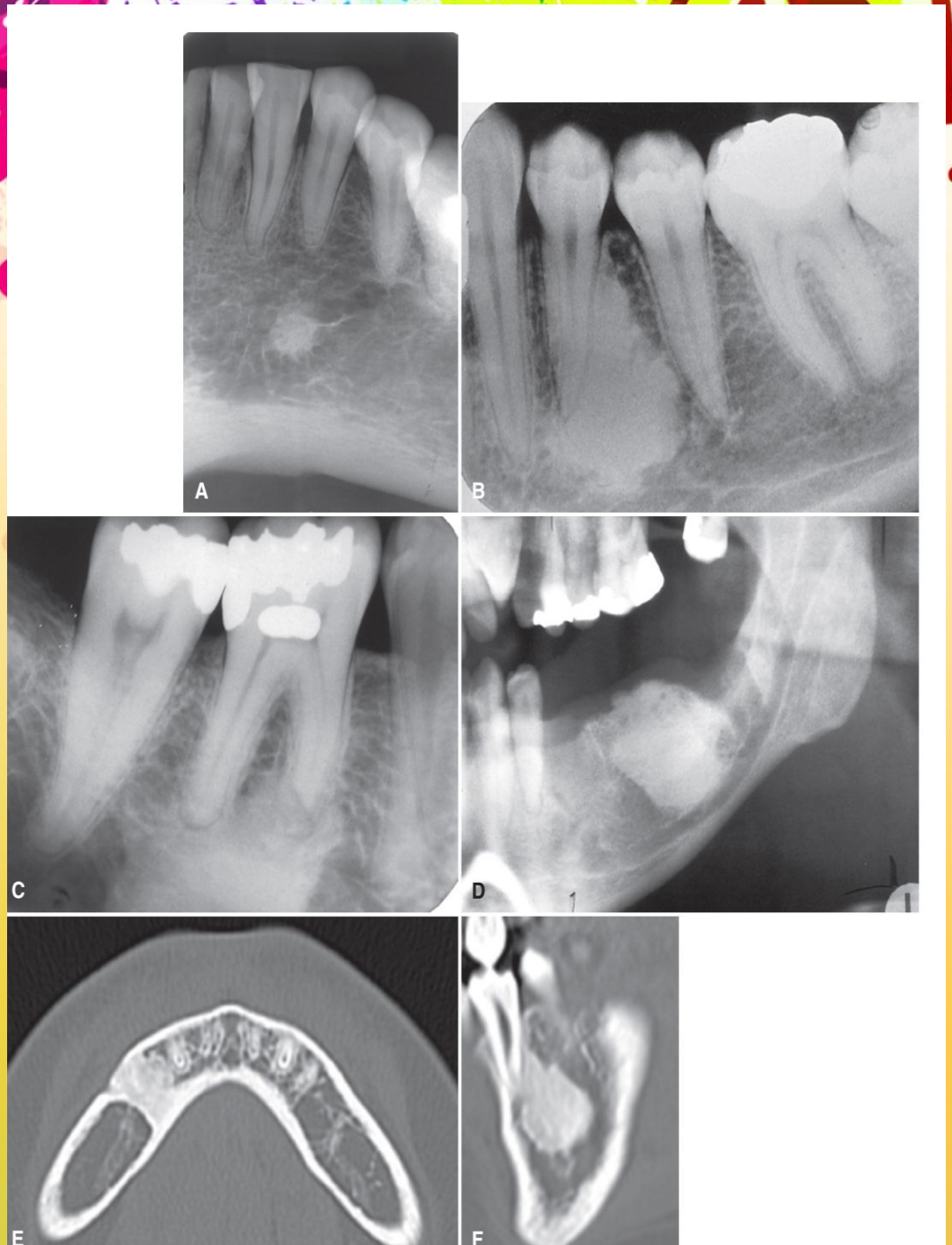
A
B
C
D
E
F

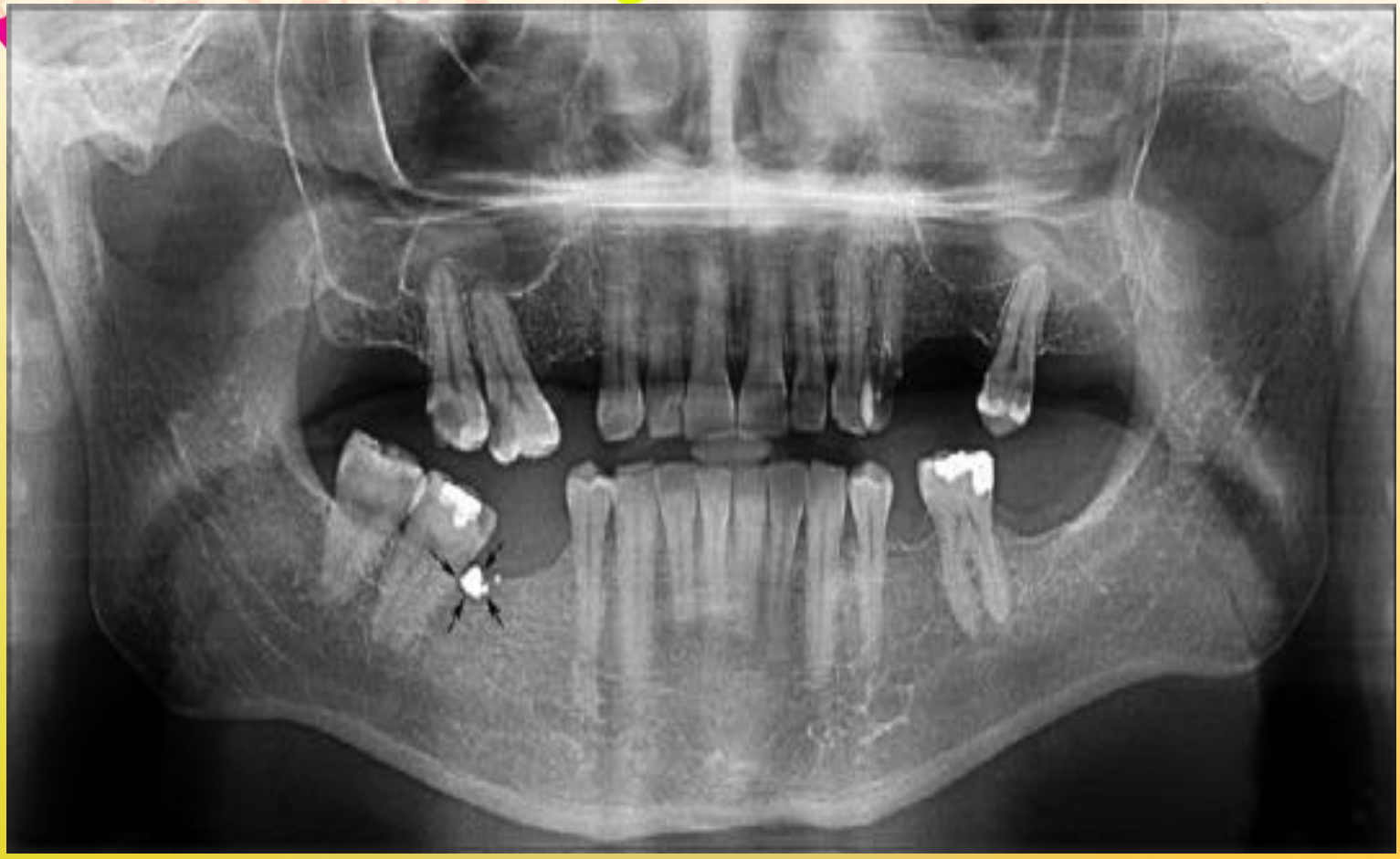

False radiopacity

- ادنتوم کامپاند
- توروس و اگزوستوز
- جسم خارجی
- موکوس ریتنشن کیست
- کلسیفیکاسیون اکتوپیک
- سیالولیت
- رینولیت و آنترولیت
- لنف نود کلسیفیه
- فلبولیت

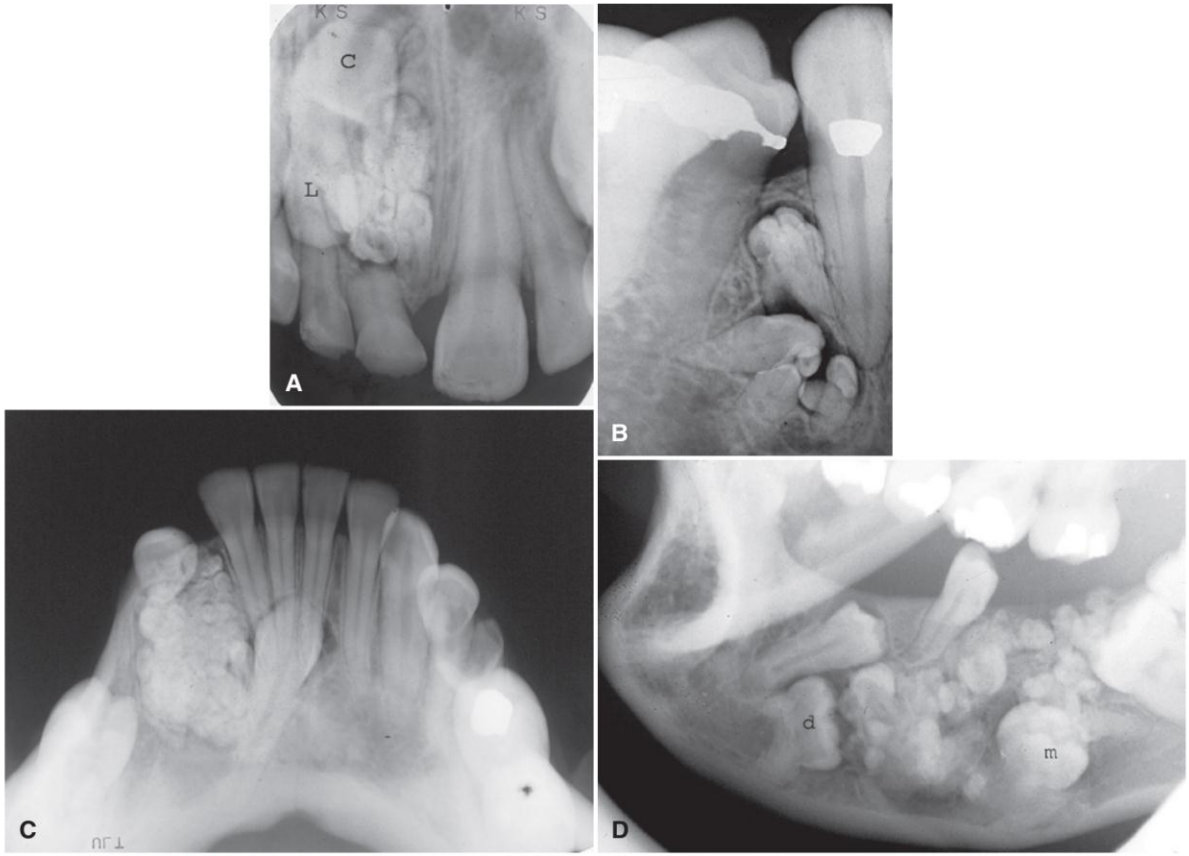

Fig. 24.20 Periapical (A and B), anterior occlusal (C), and lateral oblique (D) images of compound odontomas. Note the numerous internal, radiopaque denticles and the radiolucent periphery.

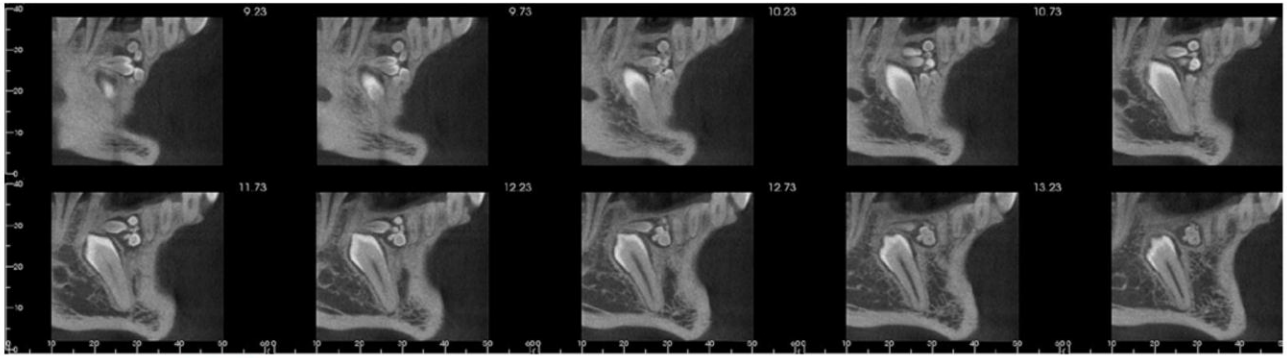

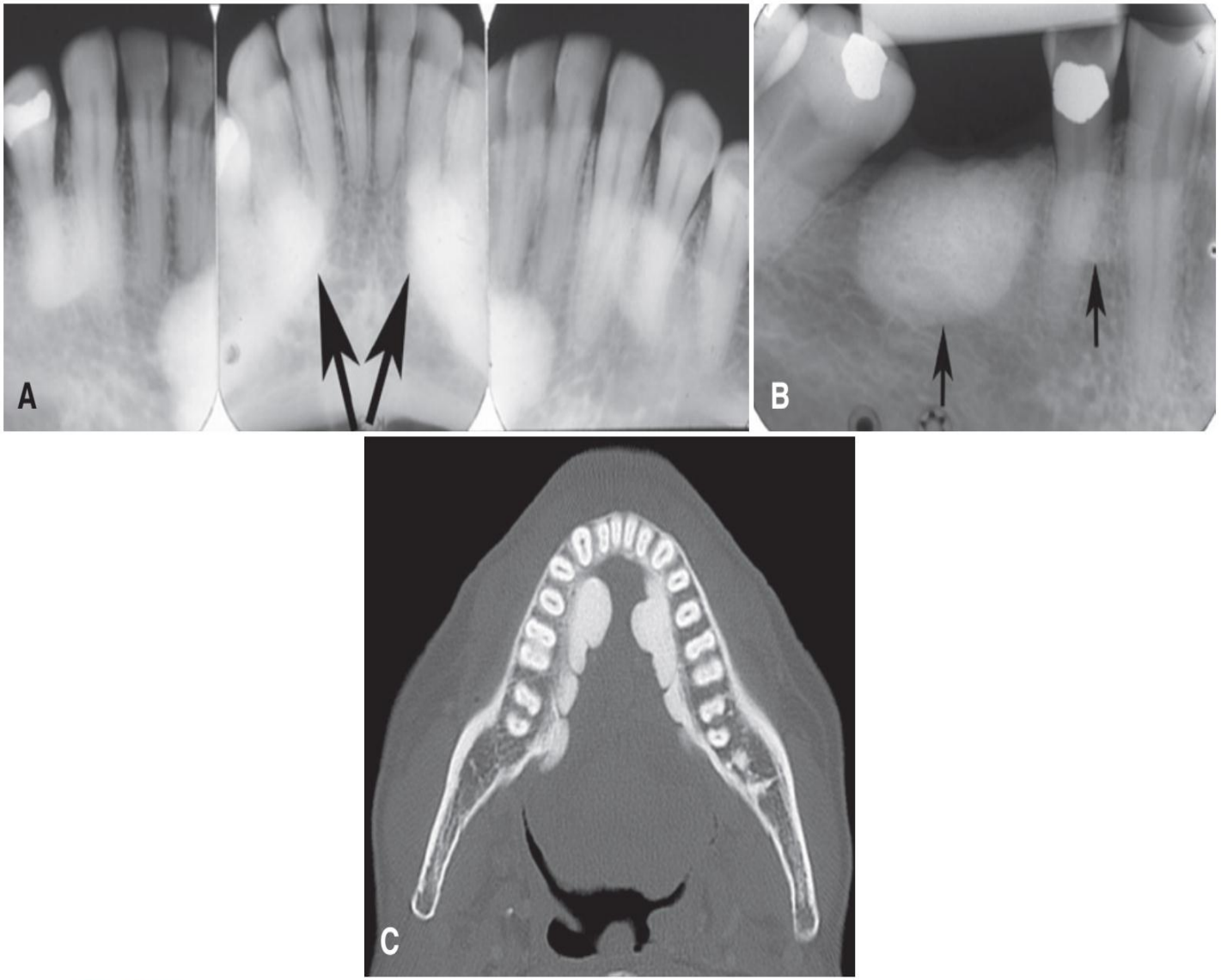

Fig. 24.39 Mandibular tori usually are seen as dense radiopacities on periapical images (A and B), superimposed over the tooth roots *(arrows)*. Axial computed tomographic image (C) with bilateral mandibular tori.

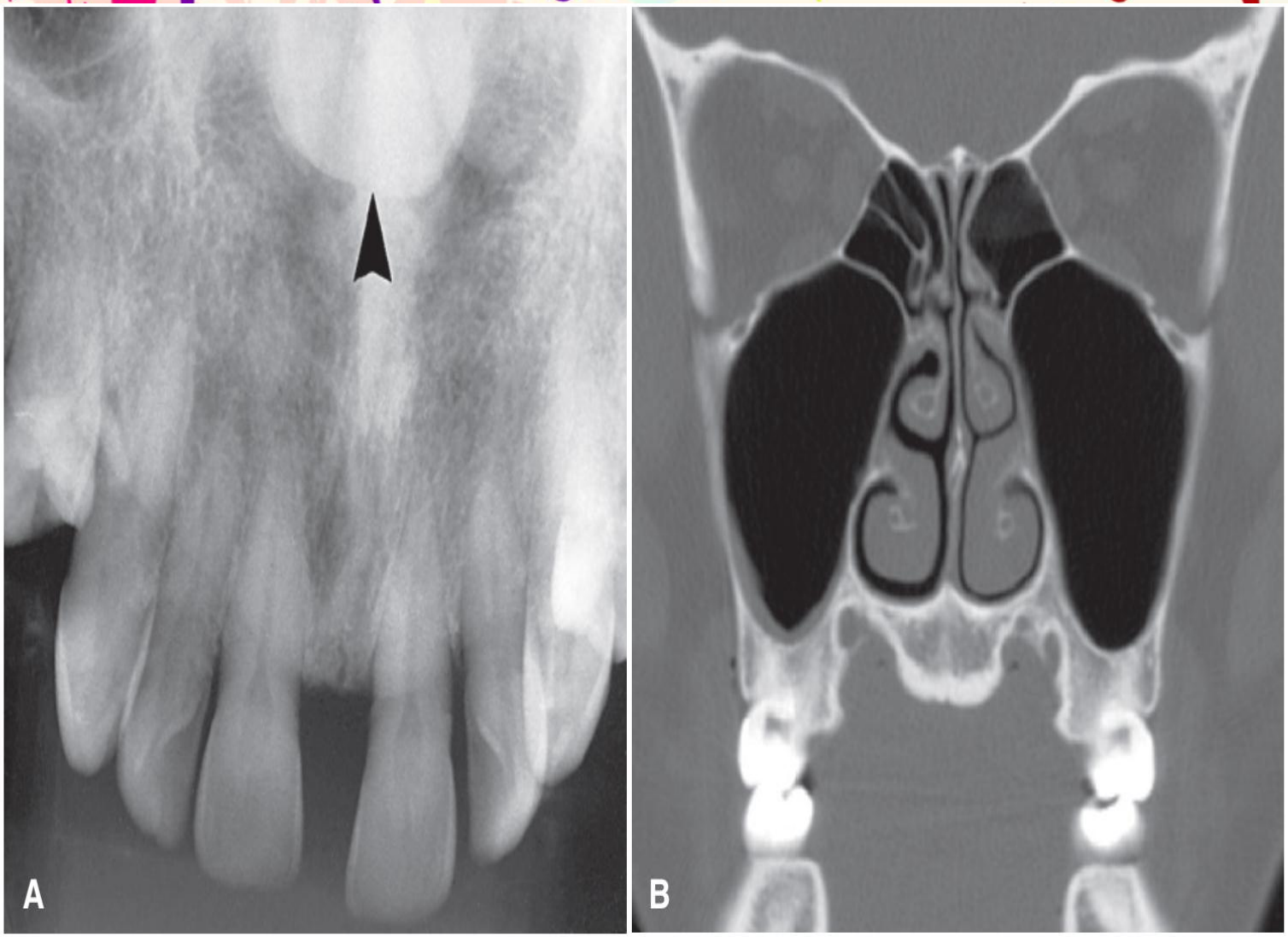

Fig. 22.40 Torus palatinus *(arrowhead)* on an occlusal image (A) and coronal cone beam computed tomographic image (B).

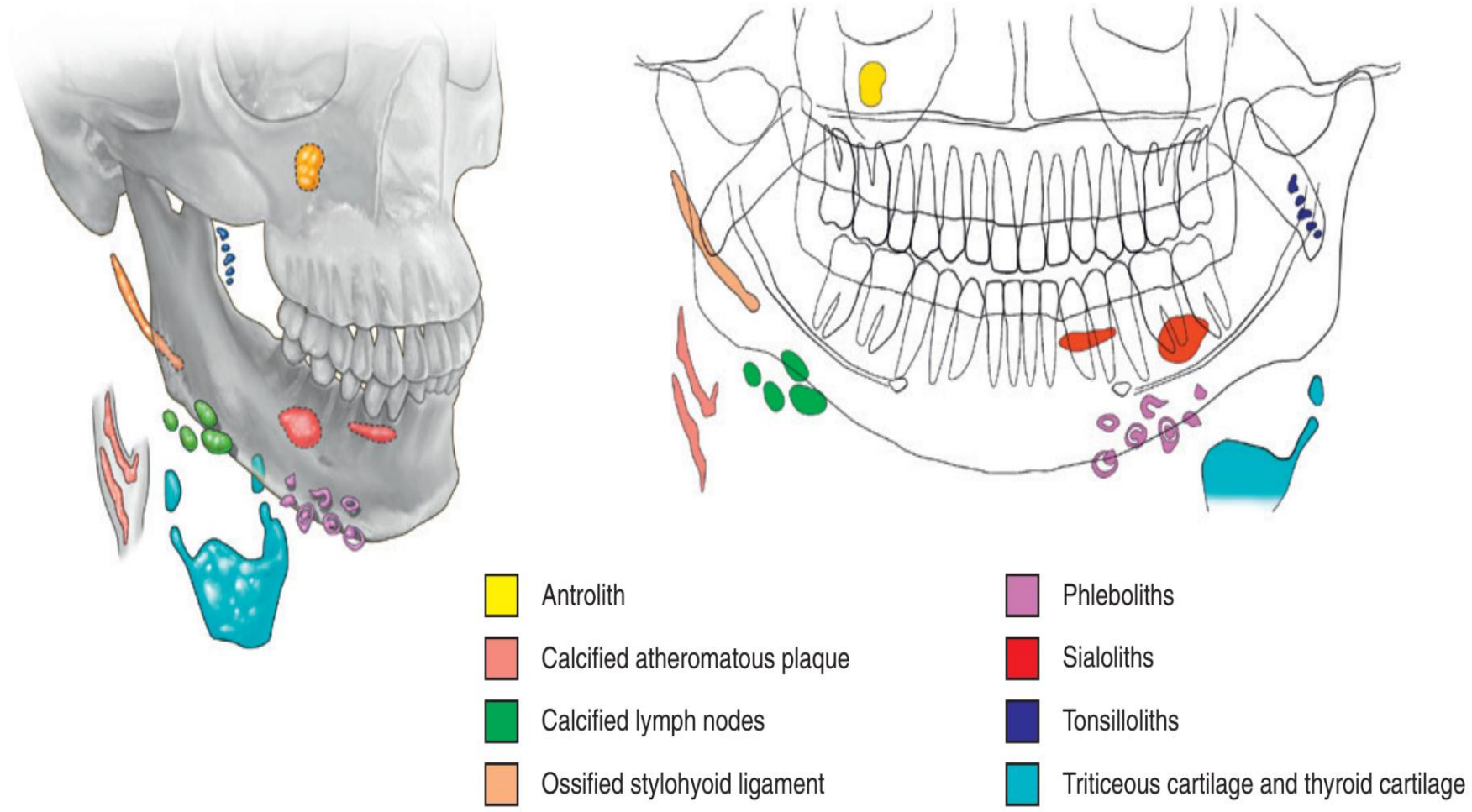

Fig. 31.1 Schematic of the head and neck, and panoramic image demonstrating the typical geometry and locations of selected soft tissue calcifications and ossifications.

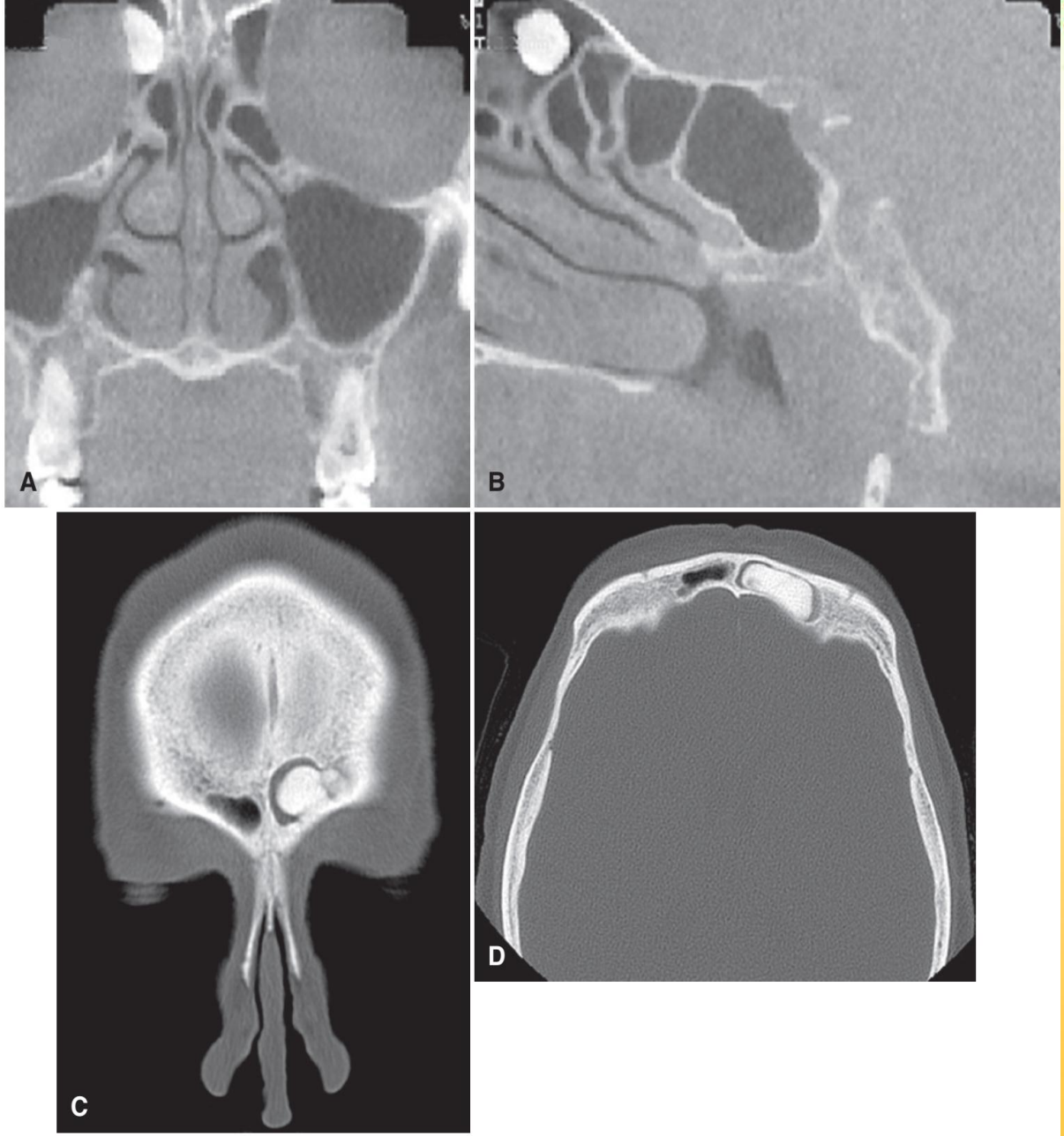

Fig. 28.13 Coronal (A) and sagittal (B) cone beam computed tomography images show an osteoma attached to the lateral wall of an anterior ethmoid air cell. Coronal (C) and axial (D) computed tomography images of an osteoma in the frontal sinus. (Courtesy Dr. E. Yu, Toronto, ON.)


A

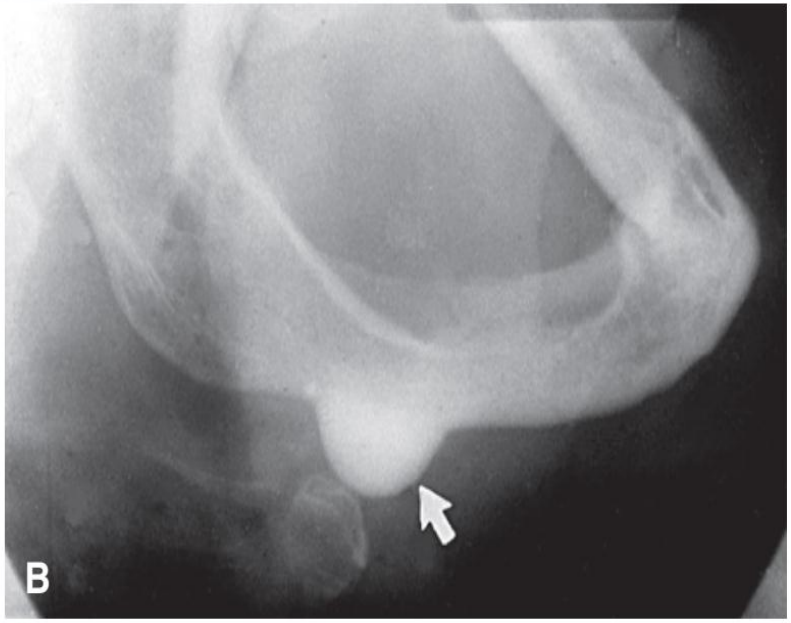
B

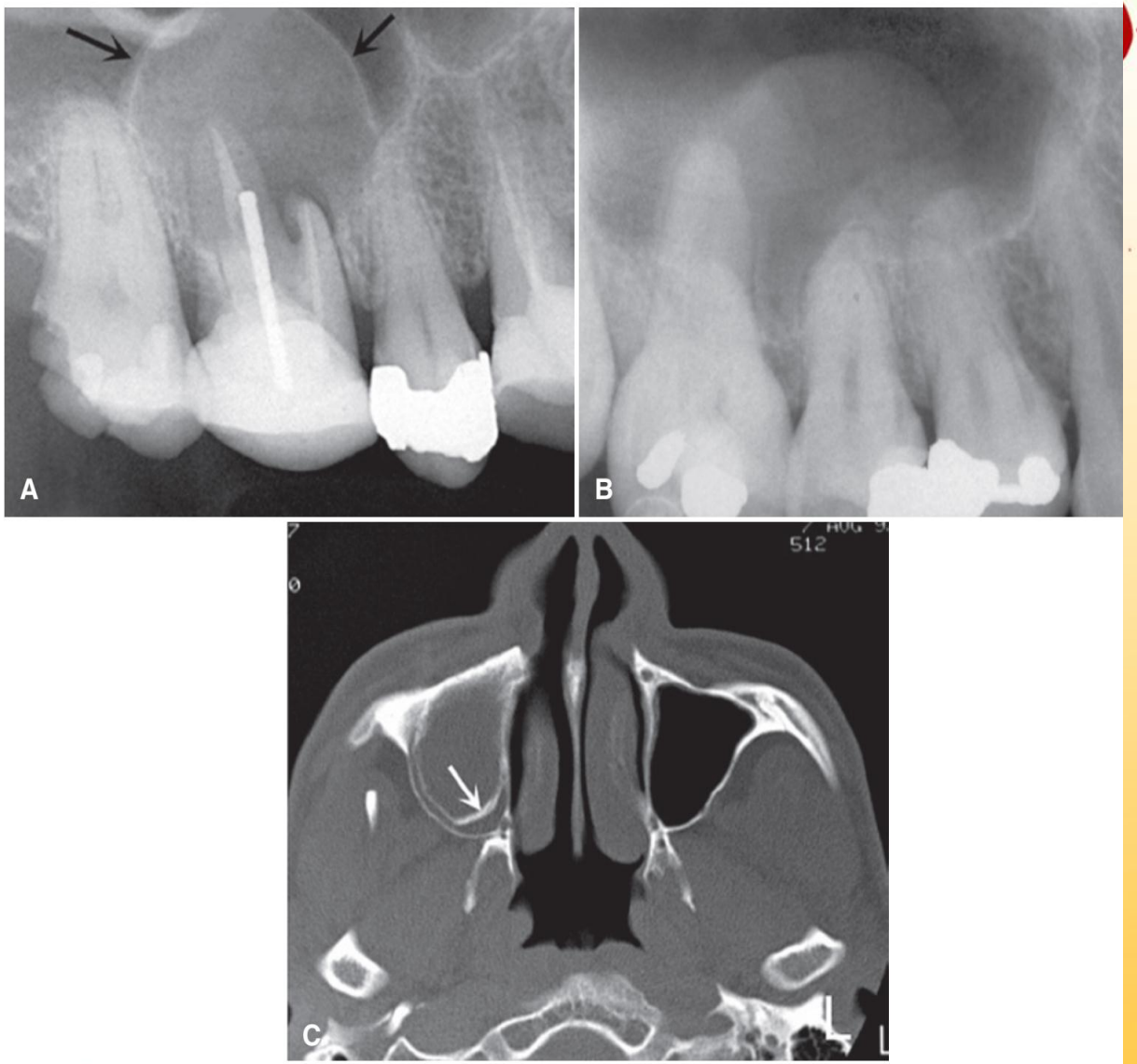

Fig. 28.17 (A) Periapical image of rarefying osteitis (in this case, a small radicular cyst) associated with a maxillary molar tooth. Note the peripheral cortex *(arrows)*. (B) Periapical image of a pseudocyst; note the lack of a peripheral cortex. (C) Axial computed tomography image of a large radicular cyst; note the peripheral cortex *(arrow)* inside the outer cortex of the sinus.

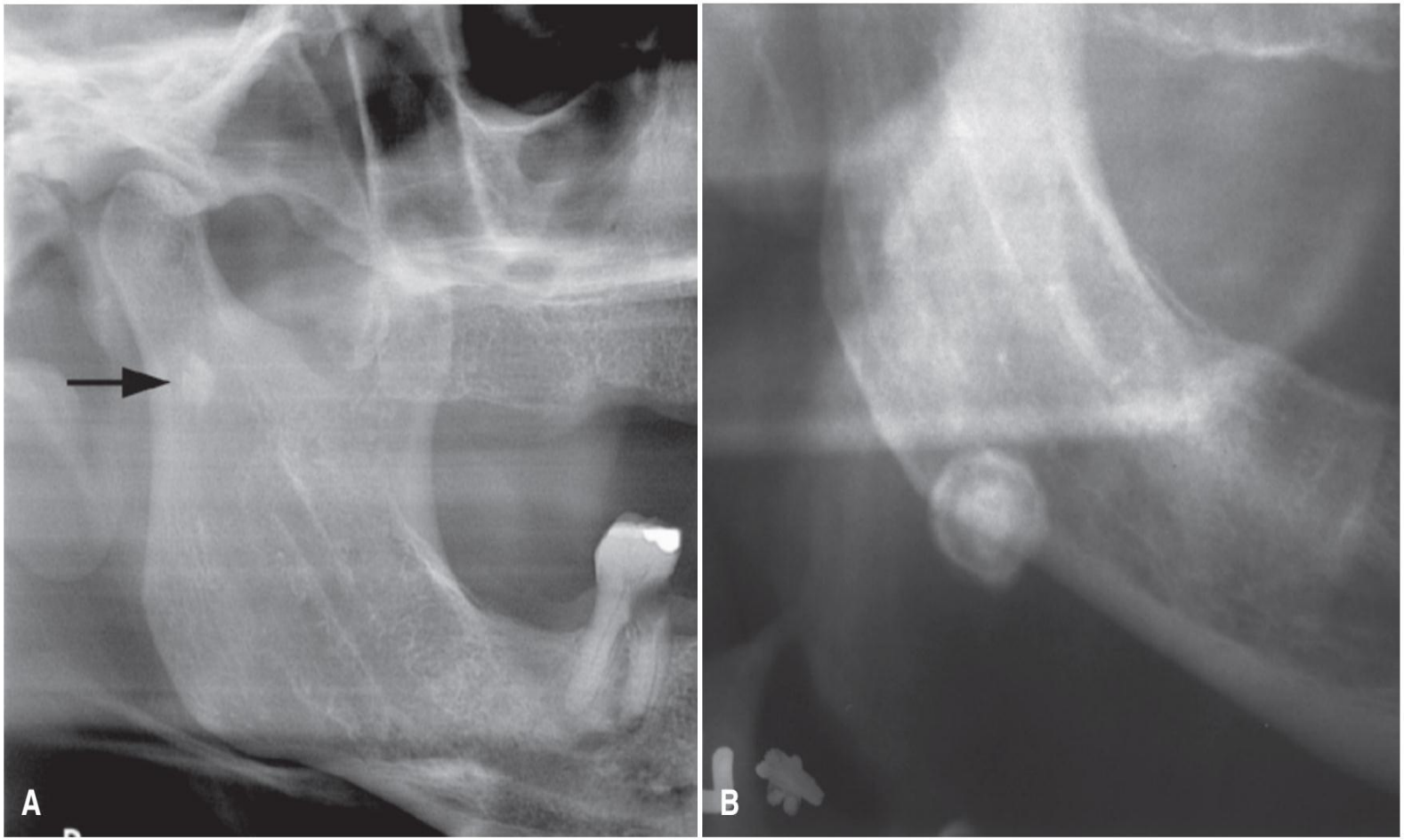

Fig. 32.3 Cropped Panoramic Images. (A) Parotid sialolith superimposed over condylar neck *(arrow)* superior to the plane of occlusion. (B) Submandibular sialolith near the antegonial notch of the mandible. Note the concentric lamellar pattern characteristic of sialoliths.

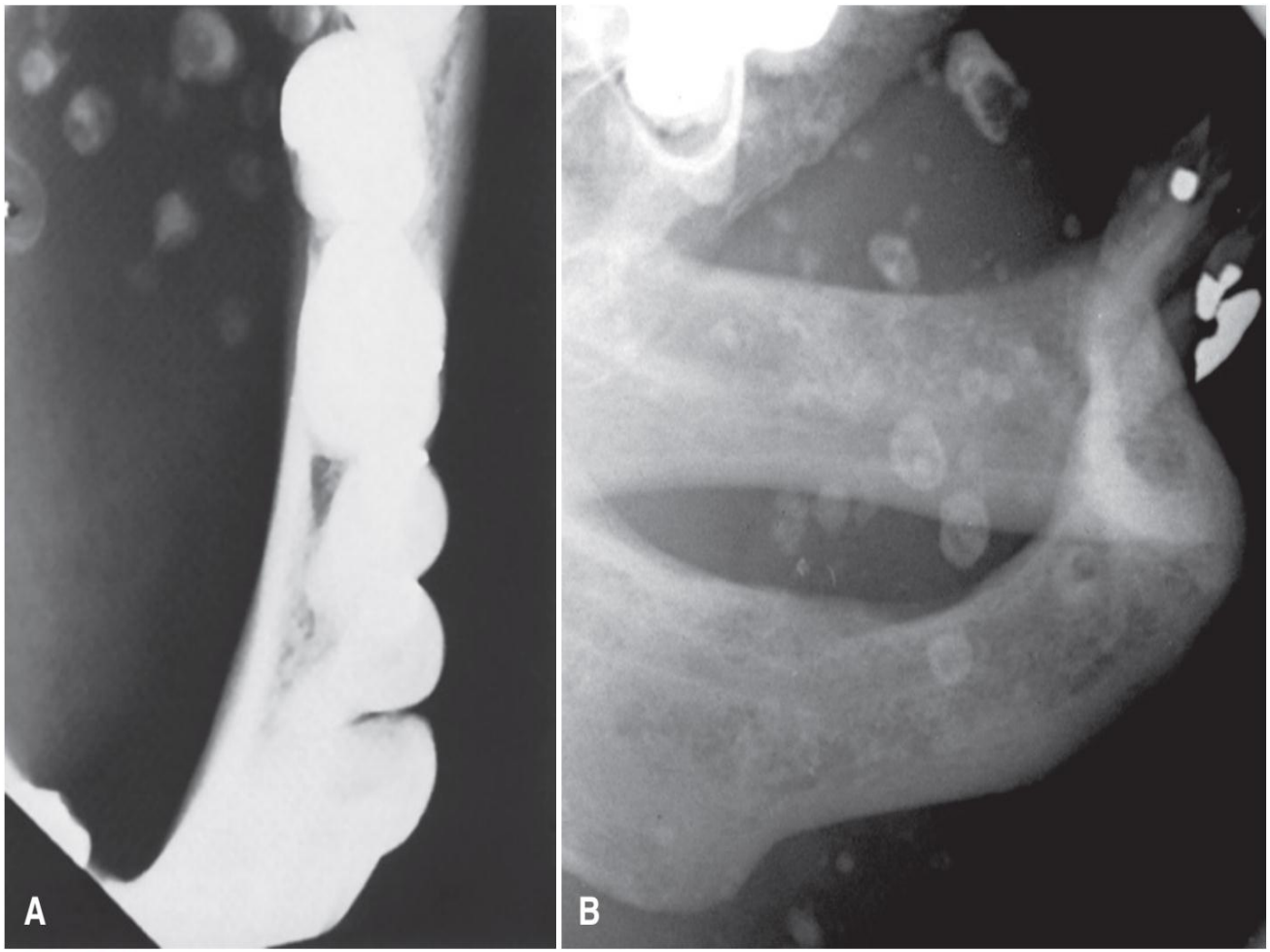

Fig. 31.8 (A and B) Phleboliths are soft tissue dystrophic calcifications found in veins. They are usually associated with hemangiomas.

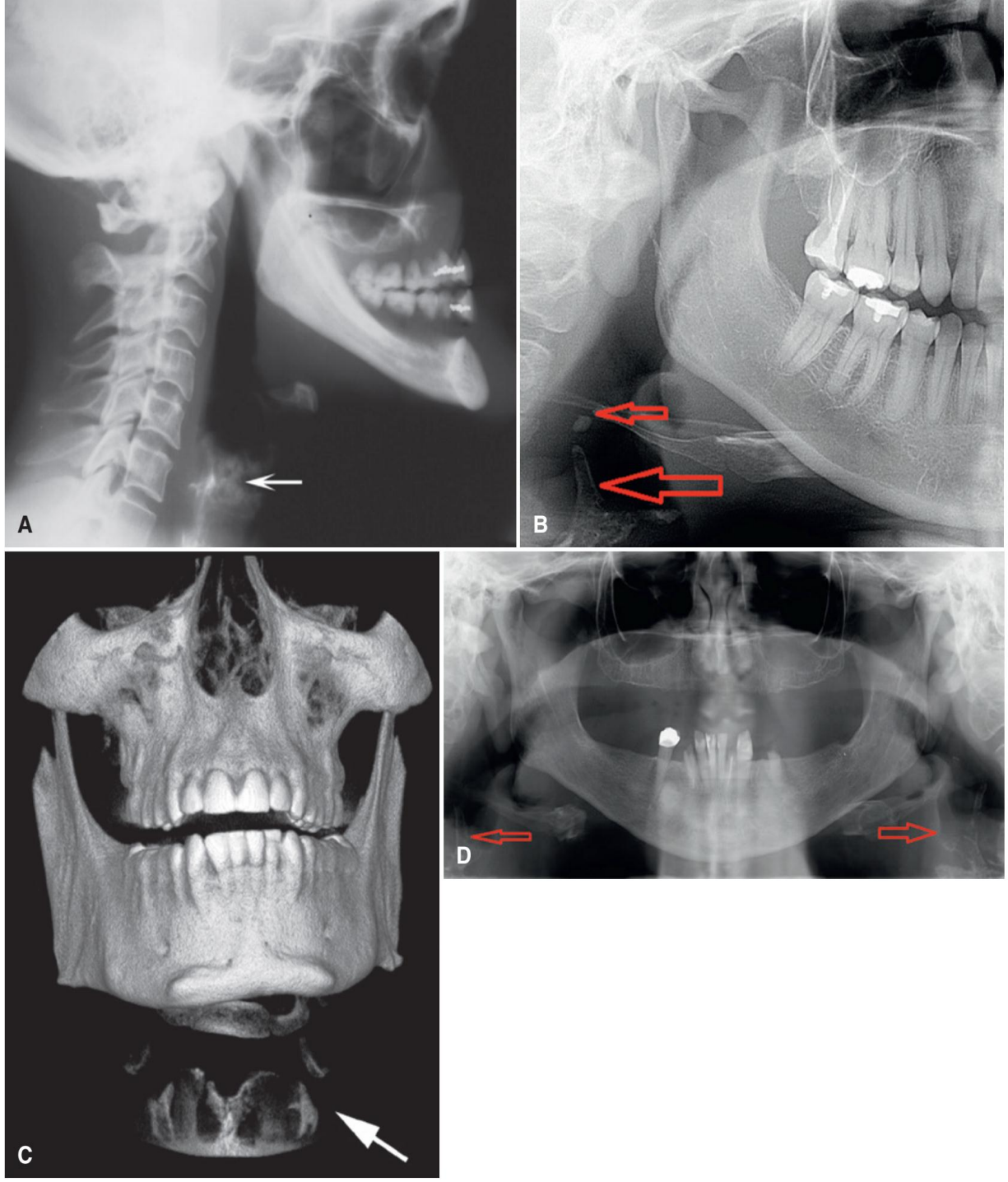
A
B
C
D

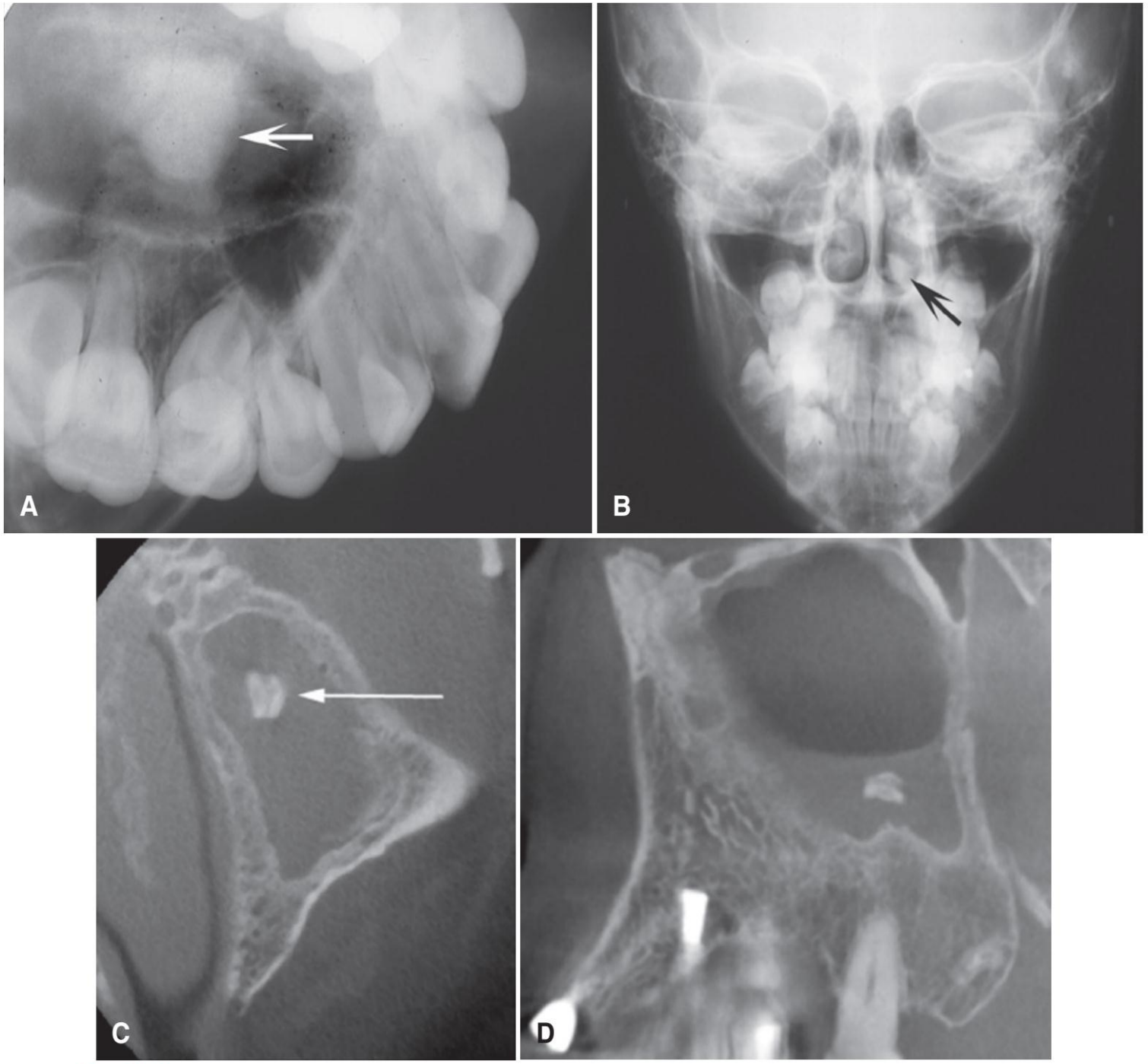
A
B
C
D


A

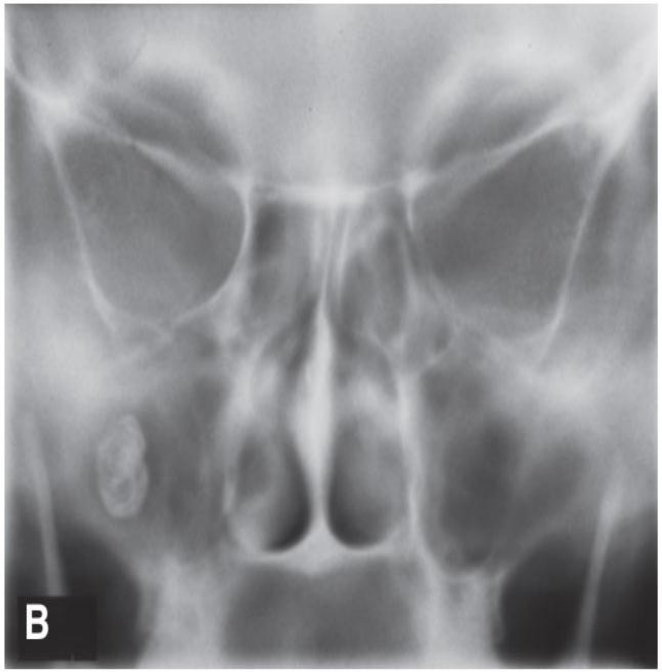
B

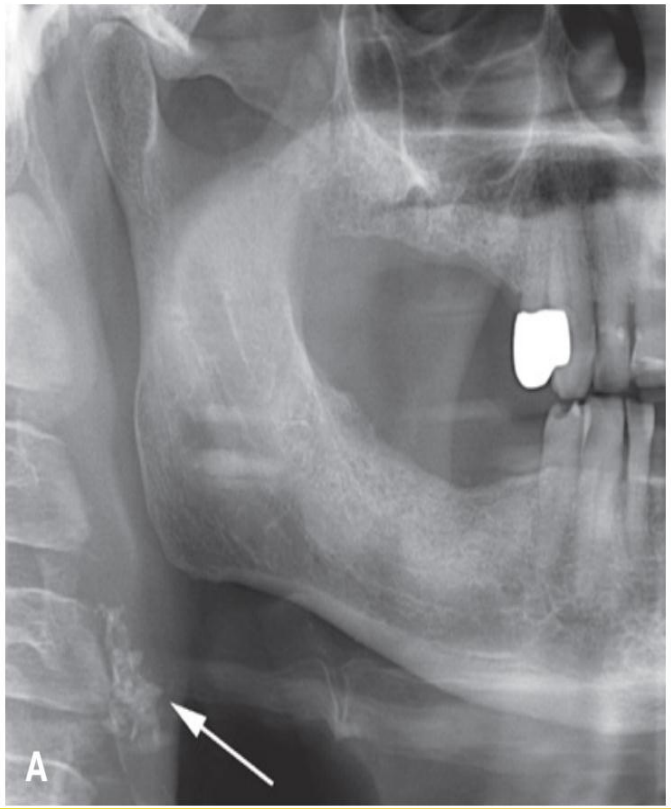
A

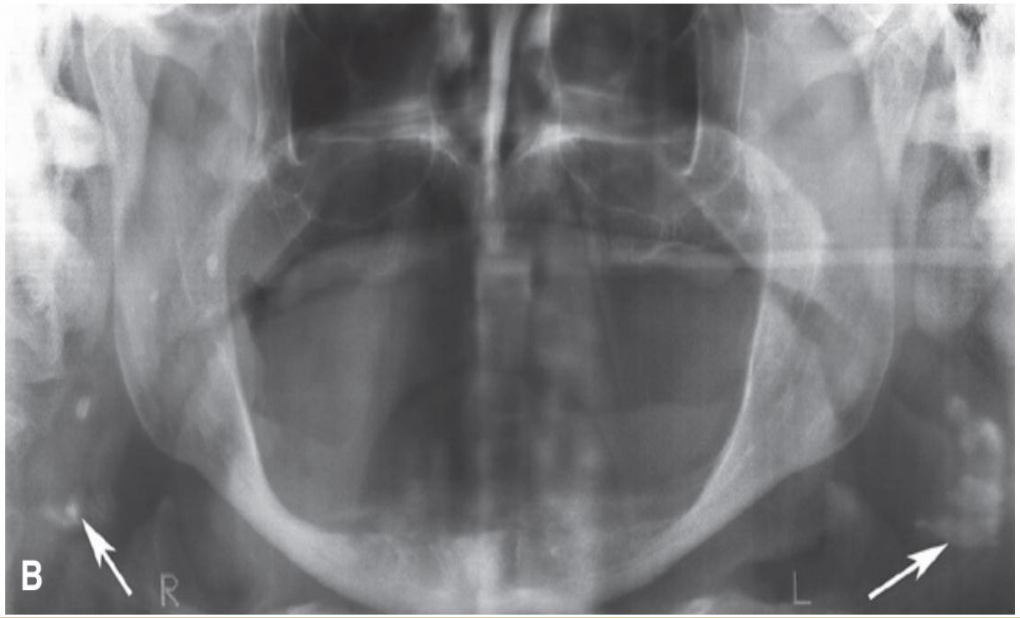
B
R
L

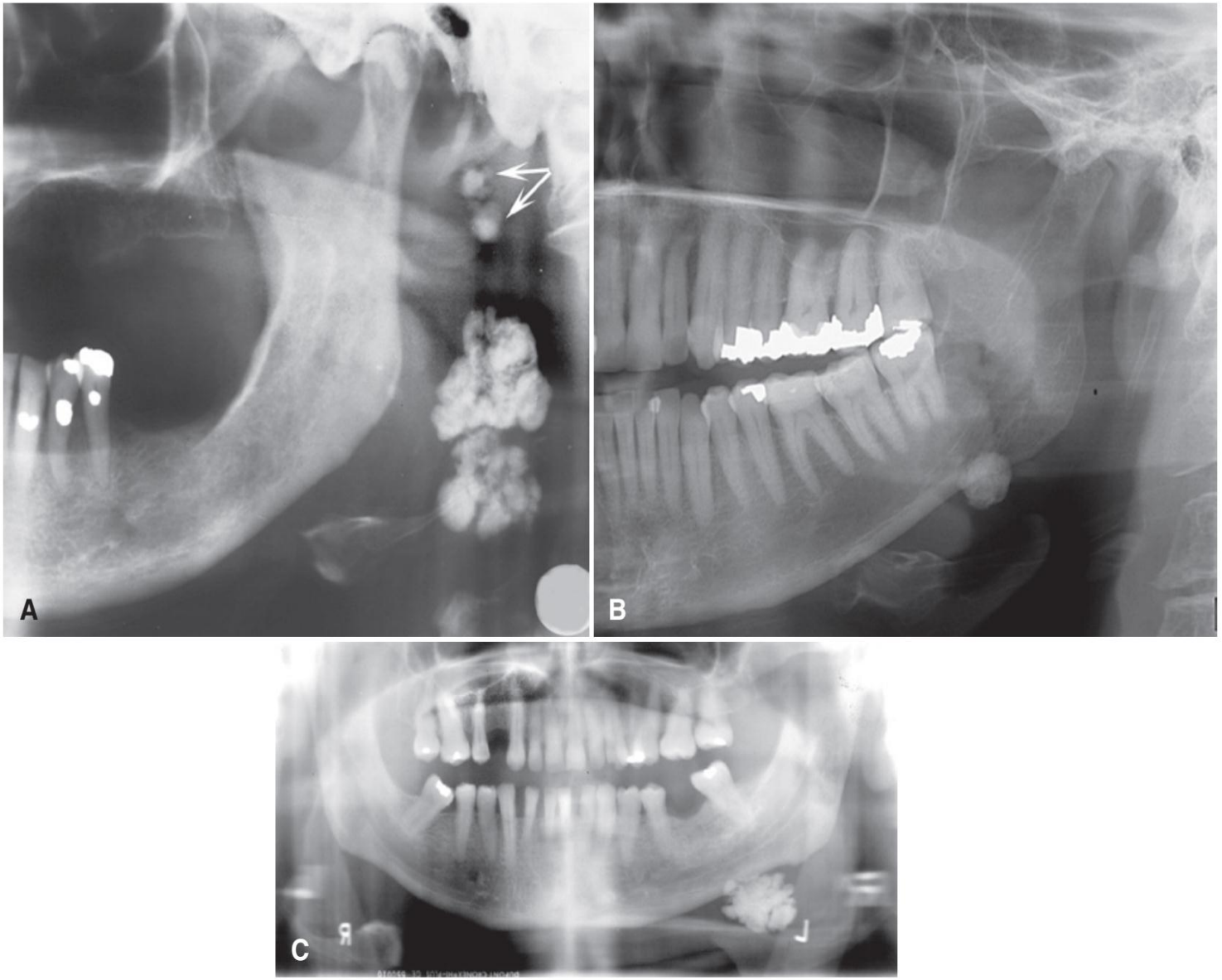

Fig. 31.4 Examples of dystrophic calcification in the lymph nodes. (A) Two large examples positioned behind the ramus with a cauliflower-like shape and two smaller examples in a more superior position *(arrows)*. (B) Submandibular lymph node superimposed on antegonial notch. (C) Larger example.

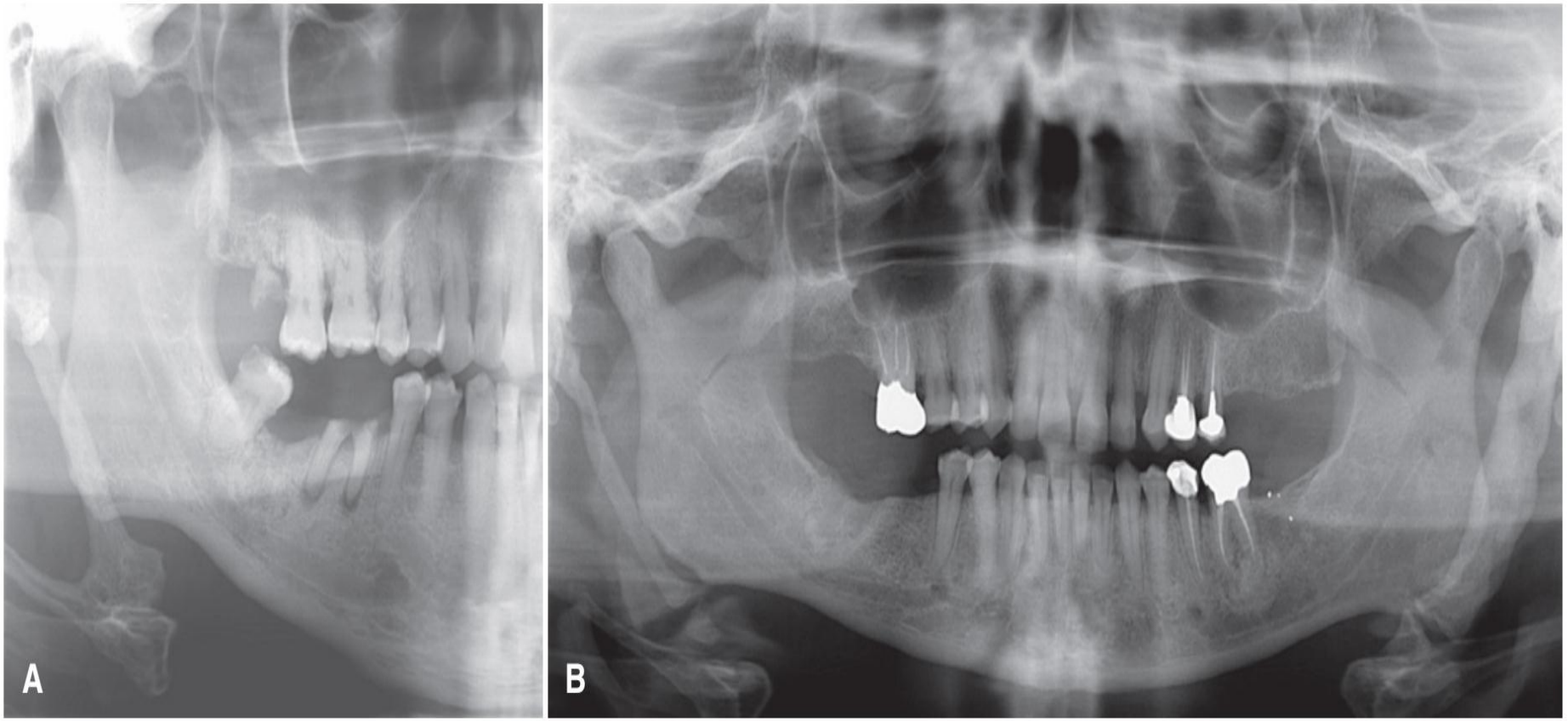

Fig. 31.11 (A and B) Examples of prominent ossification of the stylohyoid ligament. These individuals did not have any symptoms.

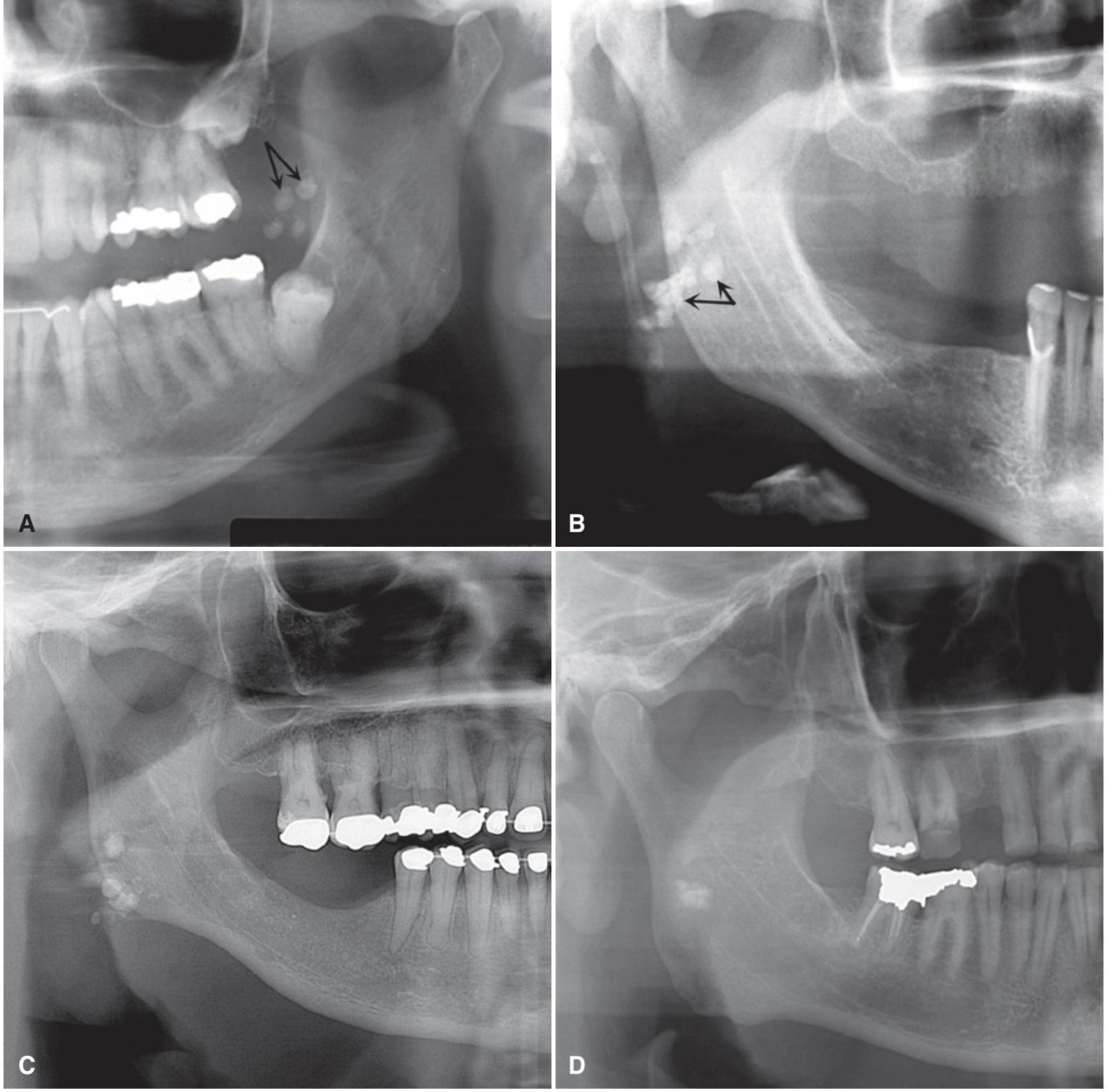

Fig. 31.5 Dystrophic calcification of the tonsils. (A and B) These two examples show positions anterior to the ramus (A) and overlapping the posterior aspect of the ramus (B; *arrows*). Note the calcified stylohyoid ligament. (C and D) Clusters of tonsilloliths superimposed on mandibular ramus.

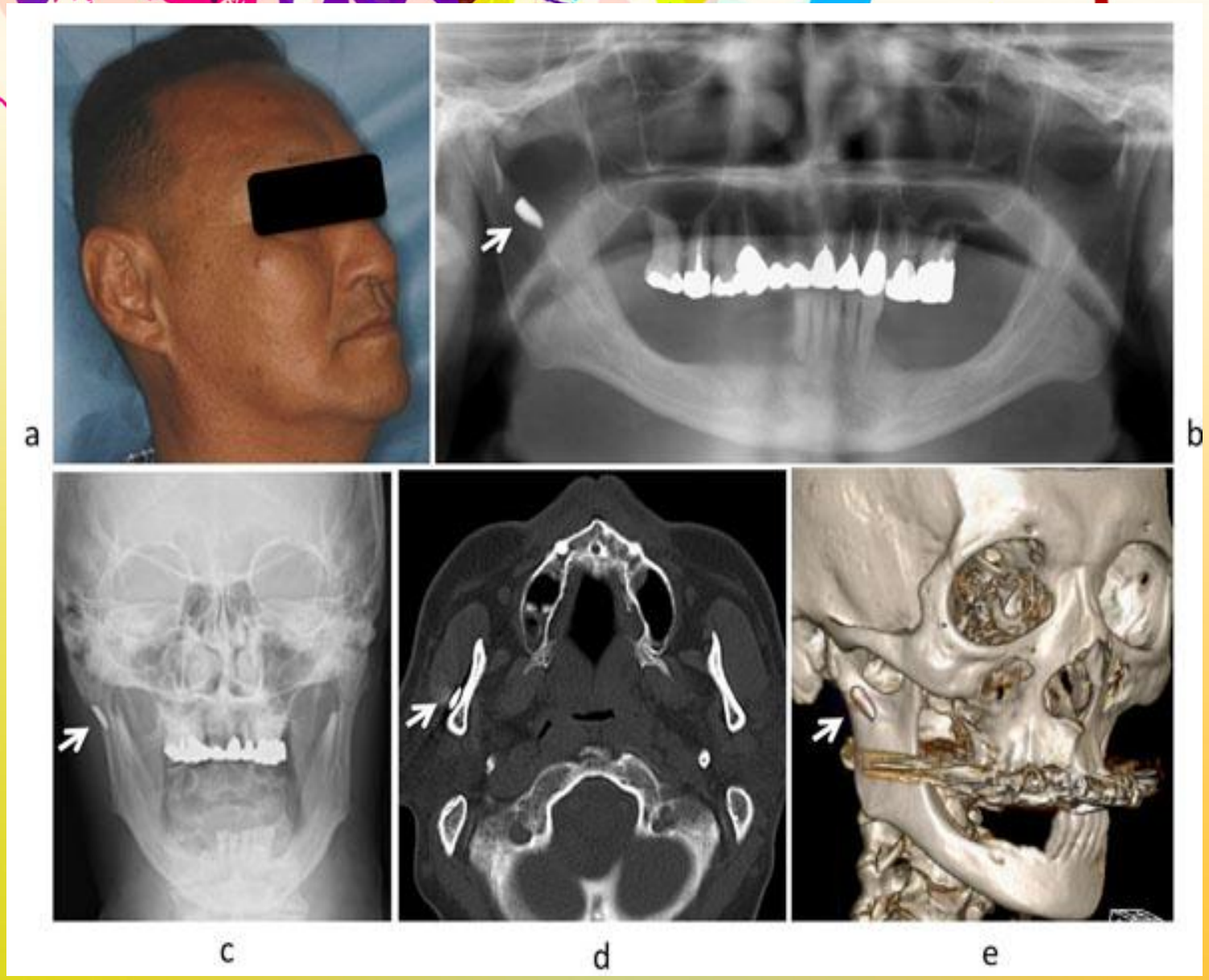
a
b
c
d
e

فیبروس دیسپلازی

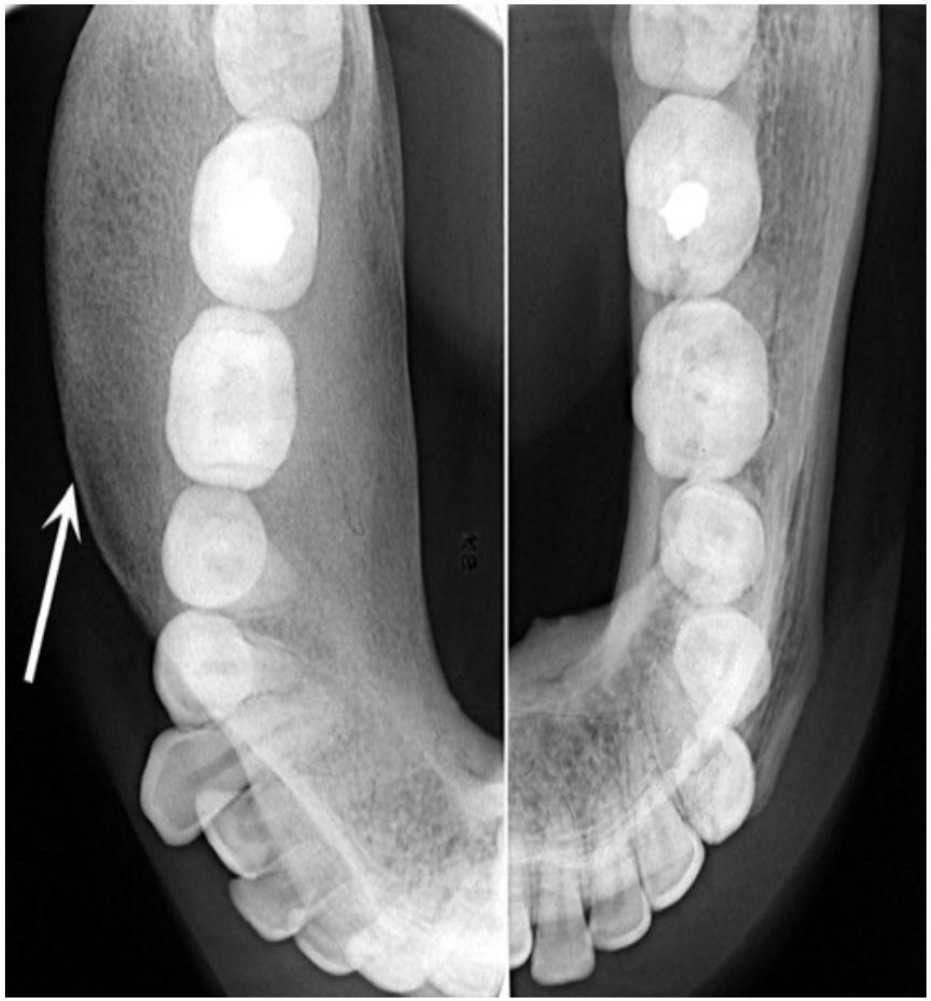

Fig. 25.34 Cross-Sectional Occlusal Images of Both Sides of the Mandible of the Same Patient. Note the expansion of the right side of the mandible, which is caused by fibrous dysplasia. The buccal surface of the mandible has been displaced, and the cortex has been thinned but is still intact *(arrow)*.


A
B
C
D

عروق كلسيفيه

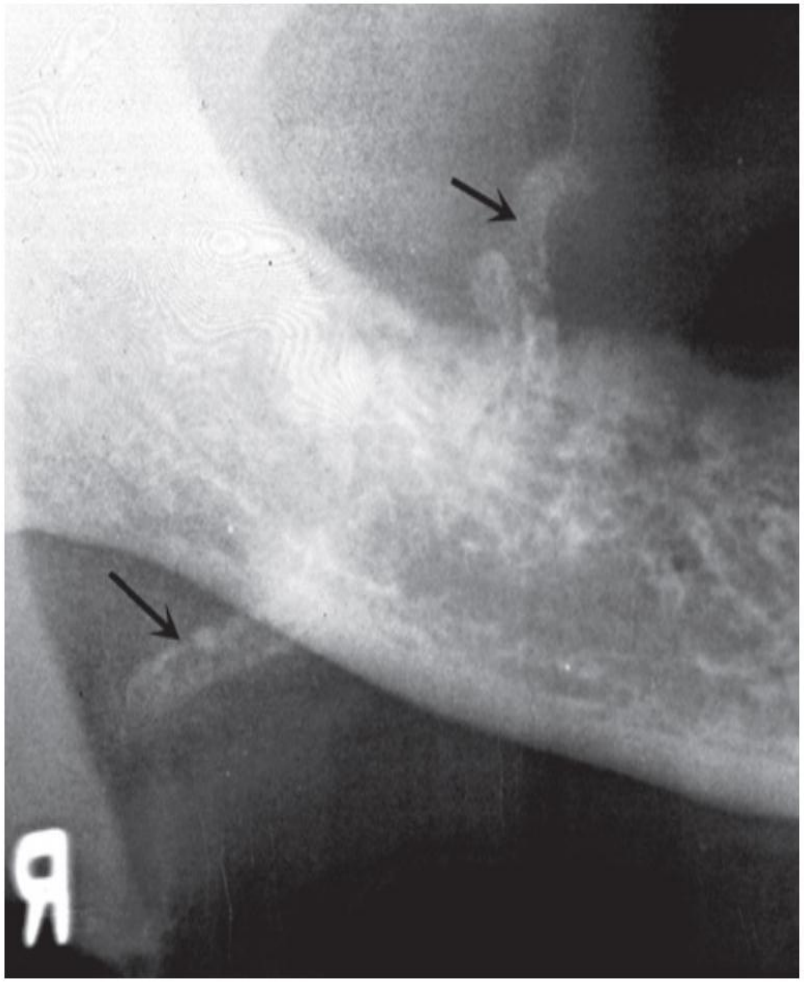

ig. 31.6 Cropped panoramic image shows calcification of a blood vessel, robably the facial vein *(arrows)*.

کمپلکس ادنتوما

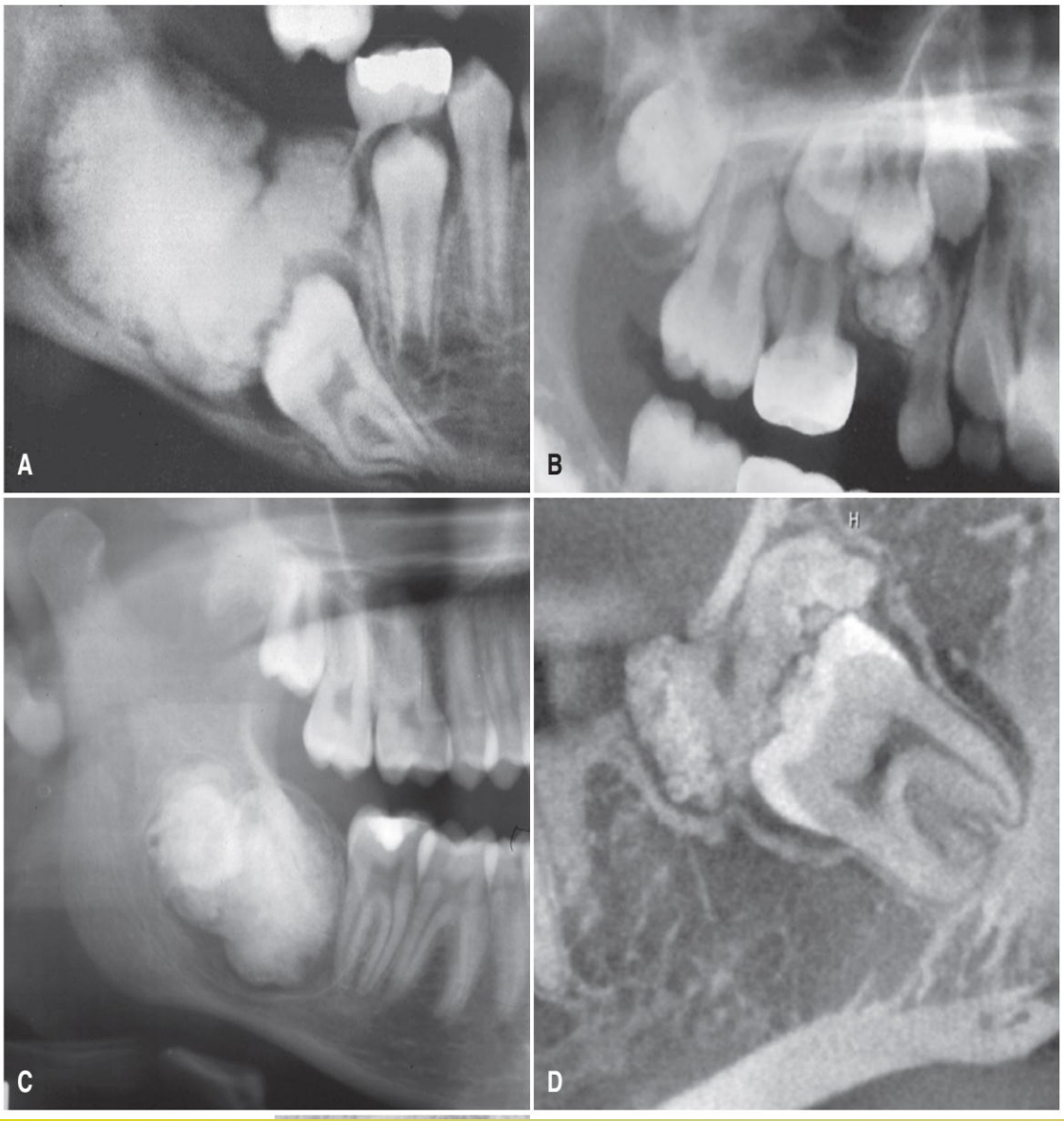

رادیواپسیتی جنرالیزه

- FLCOD
- پاژت
- استئوپتروز

Fig. 25.38 Periapical and occlusal images of Paget disease of bone showing multiple radiopaque masses in the mandible with a cotton-wool appearance (A) and mandibular expansion (B). Note maintenance of the thin cortices on the occlusal image.

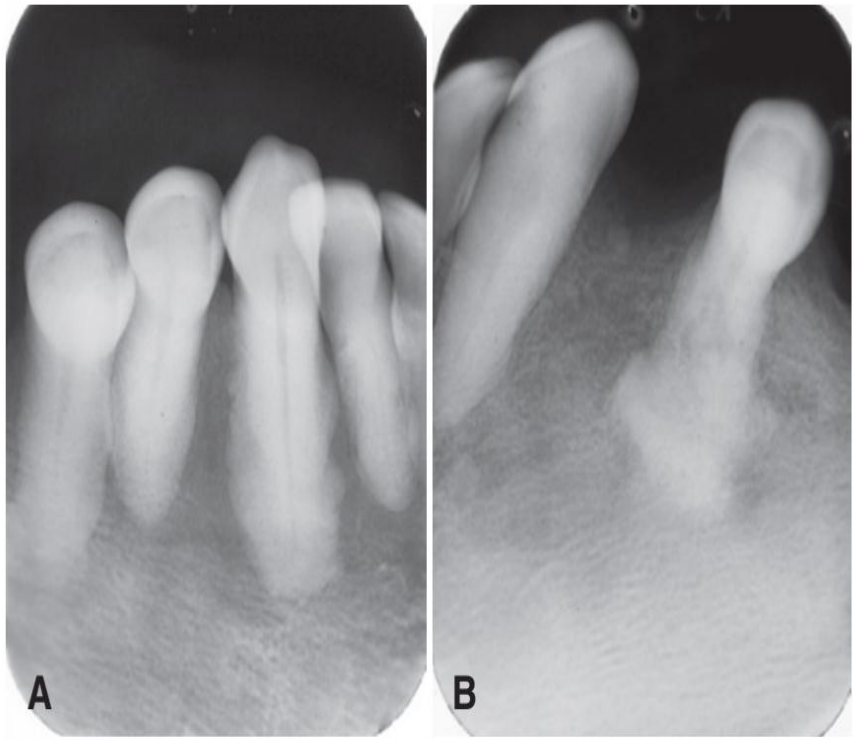

Fig. 25.39 Two periapical images Paget disease of bone showing exuberant hypercementosis of the roots.

FLCOD

ig. 25.6 A significant and generalized increase in the radiopacity of the bones is seen on this panoramic nage of a patient with osteopetrosis. The inferior alveolar canals are prominently seen and narrowed. Also, here is osteomyelitis in the body of the left mandible with periosteal new bone formation *(arrow).*